AUTICAL LABORATORIES

CALIFORNIA INSTITUTE OF TECHNOLOGY

Finite Disturbance Effect on the Stability of a Laminar Incompressible Wake Behind a Flat Plate

by

Denny R. S. Ko, Toshi Kubota and Lester Lees

HYPERSONIC RESEARCH PROJECT

Memorandum No. 72

April 15, 1969

Firestone Flight Sciences Laboratory

Guggenheim Aeronautical Laboratory

Karman Laboratory of Fluid Mechanics and Jet Propulsion

Pasadena

FIRESTONE FLIGHT SCIENCES LABORATORY

GRADUATE AERONAUTICAL LABORATORIES
CALIFORNIA INSTITUTE OF TECHNOLOGY
Pasadena, California

Finite Disturbance Effect on the Stability of a Laminar Incompressible Wake Behind a Flat Plate

by

Denny R. S. Ko, Toshi Kubota and Lester Lees

HYPERSONIC RESEARCH PROJECT

Memorandum No. 72

April 15, 1969

Contract No. DA-31-124-ARO(D)-33

U. S. Army Research Office and the Advanced Research Projects Agency

This research is a part of Project DEFENDER sponsored by the Advanced Research Projects Agency.

Ernest E. Sechler
Executive Officer for Aeronautics

ABSTRACT

An integral method is used to investigate the interaction between the stability of a single frequency finite amplitude disturbance with the non-parallel mean flow in a laminar, incompressible wake behind a flat plate. The mean flow is assumed to be characterized by a few shape parameters. The integrals involving the fluctuating components are determined as functions of those shape parameters by solving the inviscid Rayleigh equation of the linear stability theory using the local mean flow. The variations of the amplitude of the fluctuation and the mean flow in the streamwise direction are then determined from solving the set of ordinary differential equations. The effect of coupling between the mean flow and the fluctuation was found to be very important. The calculations show good agreement with the experimental data of Sato and Kuriki.

TABLE OF CONTENTS

LIST OF FIGURES

1. Introduction

The use of the infinitesimal disturbance theory of hydrodynamic stability for flow in a two-dimensional wake has been studied by McKoen, Sato and Kuriki, Gold, and others. The assumption of small disturbance allows the decoupling of the development of the disturbances from the mean flow field which is independently determined from the steady laminar equations. An exact solution for a steady laminar two-dimensional wake was obtained by Goldstein in 1933 with the additional assumption of a high Reynolds number flow. The linear stability theory further assumes a quasi-parallel mean flow, so that the disturbance equations permit a wave-like solution.

A detailed experiment for the wake behind a flat plate in an incompressible flow was reported by Sato and Kuriki in 1961, aiming at clarifying the transition mechanism in a wake. Their measurements confirmed that the initial stage of the laminar-turbulent transition can be described by the linear stability theory. They found that, in this region, the predominant disturbance was two-dimensional and antisymmetric with a frequency corresponding to the most unstable one according to the linear stability theory. However, the agreements are limited to a relatively narrow flow region near the beginning of transition. This limited range of applicability is expected because

the exponentially growing disturbances, no matter how small their initial magnitude may be, will soon invalidate the assumptions pertinent to the linearization. Sato and Kuriki found also that a fairly extensive non-linear region following the linear region existed in the wake. The following phenomena were observed in this region and are believed to be the consequences of the finite amplitude of the disturbances.

i) Two-dimensional sinusoidal fluctuations of the same frequency as observed in the linear region were still prominent. However, its growth deviated from a simple exponential rate, and the amplitude of the disturbance actually decreased in the later stage of this region.

ii) A harmonic at twice the fundamental frequency appeared with measurable amplitude which was symmetric with respect to the wake axis.

iii) The mean flow velocity and the wake width deviated substantially from the undisturbed laminar wake solution.

The present study deals with these flow behaviors when the fluctuations are still two-dimensional and dominated by a single frequency and its harmonic.

An early attempt to include the effects of a finite amplitude disturbance on the stability of flows between two parallel planes was reported by Meksyn and Stuart in 1951. The effect of the finite amplitude disturbance was introduced by including the Reynolds-stress term, $\rho\,\overline{u'v'}$, in the mean equation of motion. Only a single frequency

disturbance was considered, and the generation of the higher harmonics through the non-linear interactions between modes was ignored. Their method of solution was essentially an integral approach. The Reynolds stress was evaluated in terms of a mean flow parameter U''_0/U'_0 under the assumption that the distribution of the disturbance was given by the solution of the linearized, Orr-Sommerfeld equation, where $U_0(y)$ is the mean flow velocity and the prime denotes differentiation with respect to y. Using such an approach, they estimated the effect of the finite amplitude disturbance on the critical Reynolds number for plane Poiseuille flow. As to be expected, the results showed that the critical Reynolds number decreased as the amplitude of the disturbances increased. Stuart (1956) gave a more rigorous formulation later. The method was applied recently to the non-linear instability of plane Couette flow by Kuwabara (1967), who used the Galerkin's method to determine the mean flow and the disturbance.

An enlarged and more general formulation along this line of approach was given by Stuart (1958). In this paper, he discussed extensively the role of the Reynolds stress in determining the stability of parallel flows and the physical processes associated with the non-linearity as the disturbances grow from an infinitesimal to a finite amplitude. A Fourier series expansion was assumed for the disturbance and an assumption of constant wave velocity c_r for all the Fourier components was implied. It in turn gave the expression for the Reynolds stress, which appeared in the mean equation of motion linking the mean flow and the disturbance. An approximate

energy method was used in which the dominant non-linear interaction was assumed to be that between the mean flow and the fundamental component of the disturbance. The distribution of the disturbance was again taken from the solution of the linearized equation. The governing equation for the evolution of the amplitude as a function of time was then obtained from the integrated disturbance energy equation. This amplitude equation turned out to be of the same form as given without derivation by Landau in 1944. One most important result of Stuart's analysis is the existence of an equilibrium state when the non-linear effect is introduced. The same method was applied to the flow in a small gap between rotating cylinders. Good agreement of the torque required to maintain the cylinders in motion with G. I. Taylor's measurements was indicated.

The basic ideas of the present approach have been extracted from these works. The important difference, however, is that the streamwise variation of the mean flow is considered simultaneously with the evolution of the disturbances.

2. Formulation of the Problem

2.1 Governing Differential Equations

For the two-dimensional flat-plate wake, let x be the non-dimensional distance along the wake axis measured from the trailing edge, and y the non-dimensional distance from the wake axis. Correspondingly, u and v represent the non-dimensional velocity components. Here the reference quantities for the non-dimensionalization are chosen to be the freestream conditions and the physical plate length, L. Then the Navier-Stokes equations in two dimensions can be written as

$$\begin{aligned} u_x + v_y &= 0 \\ u_t + uu_x + vu_y &= -p_x + \frac{1}{R}(u_{xx} + u_{yy}) \\ v_t + uv_x + vv_y &= -p_y + \frac{1}{R}(v_{xx} + v_{yy}) \end{aligned} \tag{2.1}$$

where R is the Reynolds number based on the reference quantities, i.e., $R = UL/\nu$. Now, the flow is divided into a mean part independent of time and a fluctuating part with zero mean, i.e.,

$$\begin{aligned} u(x, y, t) &= \overline{u}(x, y) + u'(x, y, t) \\ v(x, y, t) &= \overline{v}(x, y) + v'(x, y, t) \\ p(x, y, t) &= \overline{p}(x, y) + p'(x, y, t) \end{aligned} \tag{2.2}$$

where the "bar" indicates a time average according to

$$\overline{Q} = \frac{1}{T}\int_{-T/2}^{T/2} Q\,dt$$

The fluctuations are assumed to be periodic in time with period T, and hence

$$\overline{u'} = \overline{v'} = \overline{p'} = 0$$

For simplicity, the time dependence of the fluctuating quantities will be assumed to be of the form $\sim e^{in\omega t}$. Here the frequency, $\omega = 2\pi/T$ is taken to be a real number, and n is an integer.

Substituting (2.2) into (2.1) and averaging over time, we obtain for the mean flow

$$\begin{aligned}
&\overline{u}_x + \overline{v}_y = 0 \\
&\overline{u}\,\overline{u}_x + \overline{v}\,\overline{u}_y + (\overline{u'^2})_x + (\overline{u'v'})_y = -\overline{p}_x + \frac{1}{R}(\overline{u}_{xx} + \overline{u}_{yy}) \qquad (2.3) \\
&\overline{u}\,\overline{v}_x + \overline{v}\,\overline{v}_y + (\overline{u'v'})_x + (\overline{v'^2})_y = -\overline{p}_y + \frac{1}{R}(\overline{v}_{xx} + \overline{v}_{yy})
\end{aligned}$$

By subtracting Eq. (2.3) from Eq. (2.1), we obtain

$$\begin{aligned}
&u'_x + v'_y = 0 \\
&u'_t + \overline{u}\,u'_x + u'\overline{u}_x + \overline{v}\,u'_y + v'\overline{u}_y + \chi_1 = -p'_x + \frac{1}{R}(u'_{xx} + u'_{yy}) \qquad (2.4) \\
&v'_t + \overline{u}\,v'_x + u'\overline{v}_x + \overline{v}\,v'_y + v'\overline{v}_y + \chi_2 = -p'_y + \frac{1}{R}(v'_{xx} + v'_{yy})
\end{aligned}$$

where

$$\begin{aligned}
\chi_1 &= u'u'_x + v'u'_y - (\overline{u'v'})_y - (\overline{u'^2})_x \\
\chi_2 &= u'v'_x + v'v'_y - (\overline{u'v'})_x - (\overline{v'^2})_y
\end{aligned}$$

For the wake flow behind a flat plate, except in the immediate vicinity of the trailing edge, the boundary-layer type approximation is

quite satisfactory for a relatively large Reynolds number. In Sato-Kuriki's experiment, the Reynolds numbers are of the order of 10^4 and higher. We will therefore consider flows of large Reynolds number and apply the boundary-layer approximation to the mean flow, which implies

i) $\overline{v}/\overline{u} = O(R^{-\frac{1}{2}}) \ll 1$

ii) b, the non-dimensional wake half-width much less than 1

iii) $\frac{\partial}{\partial x} / \frac{\partial}{\partial y} = O(R^{-\frac{1}{2}}) \ll 1$

With these approximations, if the magnitude of the fluctuation is further assumed to be infinitesimal, Eqs. (2. 3) reduce to the steady laminar wake equations

$$\overline{u}_x + \overline{v}_y = 0$$

$$\overline{u}\,\overline{u}_x + \overline{v}\,\overline{u}_y = -\overline{p}_x + \frac{1}{R}\,\overline{u}_{yy} \qquad (2.5)$$

$$\overline{p}_y = 0$$

where $\overline{p}_x$ may be set equal to zero with the boundary condition that $\overline{p}_x = 0$ as $y \to \infty$. Eqs. (2. 5) were first solved by Goldstein by joining a far-wake solution to a series expansion solution for the near-wake. This solution of Eq. (2. 5) will be referred to as the "pure laminar wake" solution in this paper.

The role of the finite amplitude disturbances can be clearly seen from Eqs. (2. 3). As the amplitude grows, the Reynolds-stress terms become comparable to the remaining terms in the equation. The rapid change in the mean flow observed experimentally in the

non-linear region indicates that the Reynolds-stress terms dominate. If A denotes a measure of the amplitude of the fluctuation, we will expect $A^2\sqrt{R}$ to be of the order one or higher in the non-linear region. In other words, when A^2 becomes $O(\frac{1}{\sqrt{R}})$, the effect of the disturbance on the mean flow can no longer be ignored. Hence, for the non-linear theory, we will keep the terms resulting from the fluctuating quantities without exact specification of their relative magnitudes as compared with the remaining terms in the mean flow equations.

Eliminating the pressure term from Eqs. (2.3), we obtain,

$$\frac{\partial}{\partial y}(\bar{u}\,\bar{u}_x + \bar{v}\,\bar{u}_y) - \underline{\frac{\partial}{\partial x}(\bar{u}\,\bar{v}_x + \bar{v}\,\bar{v}_y)} + \frac{\partial}{\partial y}\left(\overline{(u')^2}_x - \overline{(v')^2}_x\right)$$
$$+ \frac{\partial^2}{\partial y^2}(\overline{u'v'}) - \underline{\frac{\partial^2}{\partial x^2}(\overline{u'v'})} = \frac{1}{R}\frac{\partial}{\partial y}(\bar{u}_{xx}+\bar{u}_{yy})$$
$$\underline{- \frac{1}{R}\frac{\partial}{\partial x}(\bar{v}_{xx} + \bar{v}_{yy})}$$

The underlined terms in the above equation may be neglected by making the boundary layer approximation. Then we have

$$\frac{\partial}{\partial y}[\bar{u}\,\bar{u}_x + \bar{v}\,\bar{u}_y + (\overline{u'v'})_y + (\overline{u'^2}-\overline{v'^2})_x] = \frac{1}{R}\frac{\partial}{\partial y}\bar{u}_{yy} \qquad (2.6)$$

Integrating w. r. t. y from the edge with the assumption of no disturbance at the edge, we have

$$\bar{u}\,\bar{u}_x + \bar{v}\,\bar{u}_y + (\overline{u'v'})_y + (\overline{u'^2}-\overline{v'^2})_x = \frac{1}{R}\bar{u}_{yy} \qquad (2.7)$$

In principle, the complete set of the governing partial differential equations may be solved for any given flow conditions. However, it will be a difficult numerical task that will provide little understanding of the non-linear mechanism in the wake. Therefore, in an

attempt to bring out the essential effects in the non-linear region, the approximate integral method is adopted for the present investigation. In the simplest version of the integral method, the flow is required to satisfy the conservation equations of mean momentum, mean energy and fluctuation energy in integral form. These equations then lead to three ordinary differential equations for three parametric functions characterizing the mean flow and the fluctuation.

2.2 Integral Equations

The integral equations of the mean flow are obtained by integrating over the lateral coordinate y. The equations are then reduced to ordinary differential equations in x. They are

Mean Momentum Equation

$$\frac{d}{dx}\int_{-\infty}^{\infty}(\bar{u}^2 - \bar{u} + \overline{u'^2} - \overline{v'^2})\,dy = 0 \tag{2.8}$$

Mean Mechanical Energy Equation

$$\frac{d}{dx}\int_{-\infty}^{\infty}\left[\tfrac{1}{2}(\bar{u}^3 - \bar{u}) + \bar{u}(\overline{u'^2} - \overline{v'^2})\right]dy$$

$$= \int_{-\infty}^{\infty}(\overline{u'^2} - \overline{v'^2})\frac{\partial \bar{u}}{\partial x}\,dy + \int_{-\infty}^{\infty}\overline{u'v'}\frac{\partial \bar{u}}{\partial y}\,dy - \frac{1}{R}\int_{-\infty}^{\infty}\left(\frac{\partial \bar{u}}{\partial y}\right)^2 dy \tag{2.9}$$

An additional equation for the fluctuation is provided by the energy equation of the fluctuation which is obtained by multiplying the second equation of (2.4) by u' and the third one by v' and adding. This equation is then integrated over y and averaged over a period T. It yields

Mean Fluctuation Energy Equation

$$\frac{1}{2}\frac{d}{dx}\int_{-\infty}^{\infty}\left[\bar{u}(\overline{u'^2}+\overline{v'^2})+\overline{u'^3}+\overline{u'v'^2}+2\,\overline{u'p'}\right]dy$$

$$=-\int_{-\infty}^{\infty}(\overline{u'^2}-\overline{v'^2})\frac{\partial\bar{u}}{\partial x}\,dy-\int_{-\infty}^{\infty}\overline{u'v'}\left(\frac{\partial\bar{u}}{\partial y}+\frac{\partial\bar{v}}{\partial x}\right)dy \qquad (2.10)$$

$$+\frac{1}{2}\frac{1}{R}\frac{d^2}{dx^2}\int_{-\infty}^{\infty}(\overline{u'^2}+\overline{v'^2})\,dy$$

$$-\frac{1}{R}\int_{-\infty}^{\infty}\left[\overline{\left(\frac{\partial u'}{\partial x}\right)^2}+\overline{\left(\frac{\partial u'}{\partial y}\right)^2}+\overline{\left(\frac{\partial v'}{\partial x}\right)^2}+\overline{\left(\frac{\partial v'}{\partial y}\right)^2}\right]dy$$

The term $\frac{\partial\bar{v}}{\partial x}$ may be neglected as compared to $\frac{\partial\bar{u}}{\partial y}$ with the boundary-layer approximation for the mean flow. Furthermore, the term involving the second derivative in x represents the streamwise conduction of the fluctuation energy which is neglected in accordance with the boundary-layer approximation.

The advantage of the integral equations is the explicit display of the energy exchange mechanism because of the conservation forms. In Eq. (2.9), the left-hand side terms represent the variation of the mechanical energy associated with the mean flow in the flow direction, while the left-hand side terms in Eq. (2.10) give the variation of energy associated with the fluctuations. The transfer of energy between the mean flow and the fluctuations is represented by the two Reynolds-stress terms appearing on the RHS of both equations but with opposite sign. The remaining terms on the RHS of both equations represent the viscous dissipation effect.

2.3 Shape Assumption for the Mean Flow

It is the main implication of using an integral method approach

that the unknowns may be approximated by a few shape parameters which will in turn be determined by the integral equations. For the sake of simplicity, the mean velocity profiles are assumed to be characterized by two parameters; the mean velocity defect $w_c(x) = 1-\overline{u}(x, 0)$ and the wake half-width, $b(x)$. The mean velocity is then given by

$$\overline{u}(x, y) = 1 - w_c(x)\, U^*(y^*) \tag{2.11}$$

where $y^* = y/b(x)$. $U^*(y^*)$ will be assumed as known from the experiments or some other means. This complete similarity of the mean flow is not quite valid in view of the experimental results of Sato and Kuriki where overshoot of the mean velocity at some stations have been indicated. However, the profiles measured are generally close to a Gaussian distribution, and, therefore, (2.11) is a fairly good approximation throughout the transition region. A better approximation to the mean velocity can be obtained by introducing additional shape parameters such that

$$\frac{1-\overline{u}(x, y)}{w_c(x)} = U^*(y^*, H_1(x),\ H_2(x),\ ---) \tag{2.12}$$

These additional unknown parameters require additional governing equations, which may easily be obtained by using the higher moment equations.

In the equations (2.8), (2.9) and (2.10) we change the independent variables from (x, y) to (x, y^*) according to the following rules:

$$x = x$$

$$y^* = \frac{y}{b(x)}$$

$$\frac{\partial}{\partial x} = \frac{\partial}{\partial x} - \frac{y^*}{b}\frac{db}{dx}\frac{\partial}{\partial y^*} \qquad (2.13)$$

$$\frac{\partial}{\partial y} = \frac{1}{b}\frac{\partial}{\partial y^*}$$

Then, with $u^* = u'/w_c$, $v^* = v'/w_c$, and $p^* = p'/w_c^2$, together with Eq. (2.11), Eqs. (2.8) and (2.9) become

$$\frac{d}{dx}\left\{bw_c\left[(\beta_1 - \beta_2 w_c) - 2w_c(I_1 - I_2)\right]\right\} = 0 \qquad (2.14a)$$

and

$$\frac{d}{dx}\left\{bw_c^2\left[\beta_2 - \beta_3 w_c - 4w_c(I_3 - I_4)\right]\right\}$$
$$= 4w_c^3\frac{db}{dx}I_5 - 4bw_c^2\frac{dw_c}{dx}(I_3 - I_4) - 2w_c^3 I_6 - \frac{2w_c^2}{Rb}\beta_4 \qquad (2.15)$$

where

$$\beta_1 = \int_0^\infty U^*\, dy^*$$

$$\beta_2 = \int_0^\infty U^{*2} dy^*$$

$$\beta_3 = \int_0^\infty U^{*3} dy^*$$

$$\beta_4 = \int_0^\infty \left(\frac{\partial U^*}{\partial y^*}\right)^2 dy^*$$

and

$$I_1 = \tfrac{1}{2}\int_0^\infty \overline{u^{*2}}\, dy^*$$

$$I_2 = \tfrac{1}{2}\int_0^\infty \overline{v^{*2}}\, dy^*$$

$$I_3 = \tfrac{1}{2}\int_0^\infty U^* \overline{u^{*2}}\, dy^*$$

$$I_4 = \tfrac{1}{2}\int_0^\infty U^* \overline{v^{*2}}\, dy^*$$

$$I_5 = \tfrac{1}{2}\int_0^\infty y^* \frac{\partial U^*}{\partial y^*} (\overline{u^{*2}} - \overline{v^{*2}})\, dy^*$$

$$I_6 = \int_0^\infty \overline{u^*v^*} \frac{\partial U^*}{\partial y^*}\, dy^*$$

There will be an additional term of the form $[-bw_c^3 \int_0^\infty \frac{\partial U^*}{\partial x} (\overline{u^{*2}} - \overline{v^{*2}})dy^*]$ on the RHS of Eq. (2.15) when the expression (2.12) is used instead of (2.11). Without losing the main features of the present approach, we will use (2.11) throughout this paper. In this case, β_i's are constants.

Eq. (2.10) can be written as

$$\frac{d}{dx}\left[bw_c^2 \left\{(I_1+I_2) - w_c(I_3+I_4) + w_c(I_7+I_9/2)\right\}\right]$$
$$= w_c^2 I_6 - 2w_c^3 \frac{db}{dx} I_5 + 2bw_c^2 \frac{dw_c}{dx} (I_3-I_4) - \frac{w_c^2}{Rb} I_8 \qquad (2.16)$$

where

$$I_7 = \int_0^\infty \overline{u^*p^*}\, dy^*$$

$$I_8 = \int_0^\infty \left[\overline{(\frac{\partial u^*}{\partial x^*})^2} + \overline{(\frac{\partial u^*}{\partial y^*})^2} + \overline{(\frac{\partial v^*}{\partial x^*})^2} + \overline{(\frac{\partial v^*}{\partial y^*})^2}\right] dy^*$$

$$I_9 = \int_0^\infty (\overline{u^{*3}} + \overline{u^*v^{*2}})dy^*$$

The viscous dissipation integral is given approximately by I_8 after replacing the x-derivatives appearing inside the last integral of

Eq. (2.10) by its local values. That is

$$\frac{\partial}{\partial x} \approx \frac{1}{b}\frac{\partial}{\partial x^*} \quad \text{for} \quad x^* = \frac{x-x_0}{b(x)}$$

with x_0 being a reference station near x. It may be shown that the neglected terms are of the order of the square of the dimensionless fluctuation amplitude A (defined in 2.4), and this approximation introduces the same order of error as neglecting the conduction term in Eq. (2.10). Eq. (2.14a) can be immediately integrated to give

$$bw_c\left[(\beta_1-\beta_2 w_c) - 2w_c(I_1-I_2)\right] = \frac{C_D}{2} = \frac{0.664}{\sqrt{R}} \qquad (2.14)$$

where the integration constant has been obtained by assuming a laminar flow over the flat plate. It should be noted that the effect of body shape only appears through the drag coefficient C_D. Eqs. (2.14), (2.15) and (2.16) provide the governing equations for the interaction between the mean flow and the fluctuations.

2.4 Shape Assumptions for the Fluctuation

The results of Sato and Kuriki have demonstrated the dominancy of a single frequency fluctuation. Therefore, as a first-order approximation, the fluctuation is assumed to be represented by a single frequency disturbance and the generation of the higher harmonics is ignored. This assumption implies that the non-linear quadratic terms χ_1 and χ_2 in Eq. (2.4) are neglected. The remaining equations are then linear in the fluctuating quantities which, when properly normalized by the local mean flow quantities, admit a solution of the form

$$u^* = \frac{u'}{w_c} = \epsilon(x)\, f_0'(y^*;x)\, e^{i(\alpha^* x^* - \omega^* t^*)} + \text{conj}$$

$$v^* = \frac{v'}{w_c} = -i\,[\epsilon(x)\alpha^* f_0(y^*;x)\, e^{i(\alpha^* x^* - \omega^* t^*)} - \text{conj}] \qquad (2.17)$$

$$p^* = \frac{p'}{w_c^2} = \epsilon(x)\, p_0(y^*;x)\, e^{i(\alpha^* x^* - \omega^* t^*)} + \text{conj}$$

where $\alpha^* = \alpha b$ is the normalized complex wave number, $\omega^* = \omega b$, a local real angular frequency and $A(x) = \epsilon(x)\, e^{-\alpha_i^* x^*}$ measures the amplitude of the disturbance. The star indicates local variables.

Upon substituting expression (2.17) into Eq. (2.4) and neglecting all the non-local terms (e.g., $\frac{\partial \overline{u}}{\partial x}$), we obtain an equation for the distribution function $f_0(y^*)$. To further simplify the numerical analysis, we observe that a wake is dynamically unstable, and the viscous terms may be ignored for large R except for a few occasions in which the viscous terms are needed to smooth out singularity. Therefore, using the expression (2.11) for the mean flow, we obtain the Rayleigh equation for f_0,

$$(U^* - \overline{c})\left(\frac{d^2}{dy^{*2}} - \alpha^{*2}\right) f_0 - \frac{d^2 U^*}{dy^{*2}} f_0 = 0 \qquad (2.18)$$

where $\overline{c} = \frac{1}{w_c}\left(1 - \frac{\omega^*}{\alpha^*}\right)$.

The linear stability theory has indicated that an antisymmetric fluctuation is more unstable than a symmetric one as confirmed by the appearance of an antisymmetric disturbance in the experiment of Sato and Kuriki. Thus, the fluctuation is assumed to be antisymmetric which satisfies the homogeneous boundary conditions

$$f'(0) = 0$$

$$f'(y^*) + \alpha^* f(y^*) = 0, \qquad \text{as } y^* \to \infty. \qquad (2.18a)$$

Eq. (2.18), together with the boundary condition (2.18a), constitutes an eigenvalue problem. For given w_c, Eq. (2.18) can be solved numerically to obtain the eigenvalue and the corresponding eigenfunction $f_0(y^*)$. In general, for a given $U^*(y^*)$, we have

$$\alpha^* = \alpha^*(w_c, \omega^*)$$
$$f_0 = f_0(y^*; w_c, \omega^*) \qquad (2.19)$$

which indicate the functional dependence of the eigenvalue and the eigenfunction . Here we consider the spatial mode of linear stability theory, i. e. , the disturbance grows or decays spatially depending on the sign of the imaginary part of α^*.

The use of a Rayleigh equation with the local mean-velocity profile to obtain the distributions of the fluctuating components across the wake may seem to be quite arbitrary without a more rigorous analysis. At the moment, we will just note that this is merely a method of generating the fluctuation profiles in order to evaluate the required integrals as functions of the mean flow parameters and the amplitude. The integral method does not restrict the means in obtaining the distributions as long as they are good representations of the true ones. However, the use of the Rayleigh equation at least guarantees the validity in the limit of very small amplitude.

It should be noted that the formulation so far has reduced the integrals I_i to a two-parameter representation aside from the direct dependence on the amplitude A. Further approximation will now be made to simplify the analysis. We observe that, in general, the fluctuating components are much smaller than the mean-flow component,

and since both I_1 and I_2 are positive and of the same order, the contributions from the fluctuations in Eq. (2.14) may be ignored as a first approximation. This reduces Eq. (2.14) to

$$b = \frac{C_D/2}{w_c(\beta_1 - \beta_2 w_c)} \tag{2.20}$$

Then ω^* becomes a function of w_c and the integrals are simplified to be functions of a single parameter w_c when the physical angular frequency and the freestream Reynolds number are given. Of course, the validity of this assumption will have to be examined a posteriori. Thus the integrals can be written in the form

$$I_i = k_i(w_c) \left|A\right|^2 \tag{2.21}$$

for $i = 1, 2, \ldots . 8$. When only the fundamental mode is included, the triple correlations vanish and hence I_9 becomes zero.

Using Eq. (2.20), Eqs. (2.15) and (2.16) can be written as two first order ordinary differential equations for w_c and $\left|A\right|^2$ which may be solved as an initial value problem. The exact definition of A will now be given by setting

$$k_1 + k_2 = \int_0^\infty \left[\left|f_0'\right|^2 + \left|\alpha^*\right|^2 \left|f_0\right|^2 \right] dy^* = 1 \tag{2.22}$$

This definition is an appropriate one since it identifies $\left|A\right|^2$ as the averaged energy of the fluctuating components normalized by the local mean velocity defect.

2.5 Physical Mechanisms of Energy Balance

In order to bring out the physical mechanisms of the nonlinear interaction between the mean flow and the fluctuation we need consider only the leading terms in the basic equations. Later

(Section 3), these qualitative considerations are supplemented by numerical calculations using the full equations.

The integrated momentum equation (2.14), to the leading order, simply gives

$$bw_c \cong \gamma_1 R^{-\frac{1}{2}} \tag{2.23}$$

where γ_1 is a known constant of order one. The energy integral equations of the mean flow and the fluctuation to the first order, may be written as

$$\frac{dE_m}{dx} \simeq - I_6 w_c^3 - \frac{\beta_4 w_c^2}{Rb} \tag{2.24}$$

and

$$\frac{dE_F}{dx} \simeq I_6 w_c^3 - \frac{I_8 w_c^2}{Rb} \tag{2.25}$$

correspondingly. Here E_m denotes the integral energy of the mean flow. For small w_c, since bw_c is nearly constant according to Eq. (2.23), E_m is linearly proportional to w_c to the first order. E_F is the total integrated fluctuation energy given by $E_F = \int_0^\infty (\overline{u'^2} + \overline{v'^2}) dy$.

The first terms on the RHS of Eqs. (2.24) and (2.25) are the same but with an opposite sign. These terms represent an energy transfer between the mean flow and the fluctuations due to the Reynolds stress. For a locally amplified disturbance, the sign of I_6 is always positive. Therefore, the energy is transferred from the mean flow to the fluctuation through the Reynolds stress. The remaining terms on the RHS of both equations represent the effect of viscous dissipation.

Because of the growth of the wake, it is more interesting to examine the velocity defect w_c and the total energy density of the fluctuation E_T defined by

$$E_T = \frac{E_F}{b} = 2|A|^2 w_c^2 \tag{2.26}$$

Then, from Eqs. (2.21), (2.24) and (2.25), we obtain

$$\gamma_2 R^{-\frac{1}{2}} \frac{dw_c}{dx} = -k_6(w_c) E_T w_c - \frac{2\beta_4 w_c^3}{\gamma_1 R^{\frac{1}{2}}} \tag{2.27}$$

$$\frac{1}{E_T} \frac{dE_T}{dx} = \left(\frac{1}{\gamma_1} - \frac{E_T}{\gamma_2 w_c^2}\right) k_6(w_c) w_c^2 R^{\frac{1}{2}} - \frac{w_c^2}{\gamma_1}\left(\frac{k_8(w_c)}{\gamma_1} + \frac{2\beta_4}{\gamma_2}\right) \tag{2.28}$$

where γ_2 is a known constant of order one which accounts for the proportionality between w_c and E_m.

A qualitative behavior of the flow field in the non-linear region may be obtained from these two equations. When the amplitude of the fluctuation is small, the first term on the RHS of Eq. (2.27) is negligible as compared to the laminar viscous dissipation term, and the mean flow is closely approximated by the steady laminar solution, in which w_c decreases as $x^{-\frac{1}{2}}$. Since w_c changes slowly in this region, the RHS of Eq. (2.28) is approximately constant. Then, the exponential growth rate of the linear stability theory immediately follows. This region corresponds to the linear region observed by Sato and Kuriki.

As the amplitude grows, the Reynolds stress term becomes comparable with the viscous term in Eq. (2.27), and the mean velocity

defect starts deviating from the steady laminar solution. As the fluctuation is further amplified, the Reynolds stress term becomes dominating. The experimentally observed rapid change of the mean velocity and the wake width in the non-linear region may be understood from this consideration. From the solution of the Rayleigh equation we learn that the local amplification rate decreases as w_c decreases if a single fixed frequency fluctuation is followed. Hence, when the fluctuation corresponding to the most unstable frequency in the linear region is taken to represent the fluctuating component, it will approach neutral as w_c decreases. Thus, when w_c decreases to the value where k_6 becomes small, the mean flow is expected to have a relatively slow variation, as observed experimentally.

The qualitative behavior of the fluctuation in the non-linear region may be deduced from Eq. (2.28). For $k_6 >> R^{-\frac{1}{2}}$, the first term dominates. The appearance of the E_T term with a negative sign on the RHS of Eq. (2.28) is the most interesting feature caused by the growth of the wake. It permits not only a state where $dE_T/dx = 0$, but also a decreasing E_T with x even when the fluctuation under consideration is still amplifying according to the local linear theory ($k_6 > 0$). Experimentally, the maximum amplitude of the fundamental mode grows initially but decreases after reaching a peak value. This fact may now be explained since the energy density E_T is expected to be indicative of the magnitude of the fluctuation.

The crucial differences of the present problem from the parallel flow analysis of Stuart (1960) and Watson (1960, 1962) become evident from the above discussions. The main result of the non-linear analysis

of Stuart and Watson is the governing equation for the amplitude of the disturbances, which is of the form

$$\frac{1}{|A|^2}\,\frac{d|A|^2}{dx} = \bar{a}_0 + \bar{a}_1\,|A|^2 + \text{----} \qquad (2.29)$$

where $\bar{a}_n$'s are constants. The coefficient $\bar{a}_0$ is given by the linear theory with the undisturbed laminar mean flow, and $\bar{a}_1$ is a result of three effects: the generation of the second harmonic, the correction of the fundamental and the correction to the laminar mean flow. The amplitude $|A|$ in the Stuart-Watson theory corresponds to the average energy density E_T defined by Eq. (2.26). Then, an analogous equation of the form of Eq. (2.29) results with $|A|^2$ being replaced by E_T. However, the coefficients $\bar{a}_0$ and $\bar{a}_1$ are no longer constants but functions of x through the variation of the mean flow. Since the mean flow is not expanded as the undisturbed laminar flow plus a correction in the present problem but is lumped together to be determined by the integral equations, the so-called second Landau constant does have an appreciable magnitude even when the second harmonic is ignored. The sign of $\bar{a}_1$ is opposite to that of $\bar{a}_0$. In the case of a parallel flow, a supercritical equilibrium state may exist. However, the continued variation of the mean flow provides the possibility of a decreasing magnitude of the fluctuation before reaching the final equilibrium state as demonstrated previously.

3. Results and Discussion

For the purpose of comparison with the experimental results of Sato and Kuriki, the numerical calculations have been performed corresponding closely to the experimental conditions. The mean velocity function, $U^*(y^*)$, used for the calculation is taken to be the one used by Sato and Kuriki in the linear region, i. e.,

$$U^*(y^*) = \exp(-0.69315\ y^{*2}) \tag{3.1}$$

Eq. (3.1) also gives the exact definition of the half-wake width b as the distance from the wake axis to the half velocity defect point where $U^* = 0.5$. The frequency of the fundamental mode used in the calculation is also taken from the experiment of Sato and Kuriki to be 730 cps at $R = 2 \times 10^5$. This frequency was found to be the one receiving nearly maximum amplification rate in the linear region given by the temporal mode calculation of Sato and Kuriki.

With the frequency fixed at this value, the variation of the local amplification rate was determined as a function of the mean velocity defect w_c by solving the Rayleigh equation as formulated in 2.4. The result shows that the amplification rate decreases as w_c decreases. At $w_c \approx .147$, $\alpha_i^* = 0$; the given frequency corresponds to a neutrally stable solution according to the linear stability theory. Further decrease of the mean flow parameter w_c will make this frequency a damped disturbance ($\alpha_i^* > 0$) according to the linear theory.

The integrals k_i as functions of w_c were then computed from the eigensolutions of the Rayleigh equation . After this preparatory

computation, the integral conservation equations were integrated for each given set of initial conditions to determine the simultaneous evolutions of the mean flow and the fluctuation.

3.1. Comparison with the Experiment

Most of the experimental results presented by Sato and Kuriki were obtained with a freestream velocity U = 10m/sec. and a plate length L = 30 cm. These conditions correspond to a freestream Reynolds number of 2×10^5. From the experimental evidences, the wake was steady and laminar for a short distance from the trailing edge of the plate. The calculations are therefore started at an initial station $\zeta_0 = .05$ using the appropriate initial conditions. The center-line velocity defect w_{c0} at ζ_0 can be taken from either the exact solution of Goldstein or the integral solution of an undisturbed laminar wake in the present formulation. The latter is not very accurate there, since the velocity distribution deviates from the Gaussian as ζ_0 decreases. For the present comparison purposes, it was decided to use $w_{c0} = 0.7$ at $\zeta_0 = .05$ from the exact solution of Goldstein because of the closer agreement with the experiment at that point. Another initial parameter is the initial integrated energy content in the u'-component; i.e.,

$$E_{u0} = \left(\frac{1}{b}\int_0^{\infty} \overline{u'^2}\, dy\right)_0 \qquad (3.2)$$

where the subscript "0" refers to value at ζ_0. The value of this parameter depends on the different flow conditions encountered in each experiment, e.g., the freestream turbulence intensity level, the physical dimension of the plate trailing edge, etc. In the present

study these two initial parameters were chosen somewhat arbitrarily in performing the following calculations. The effects of each of the initial parameters on the complete solutions will be investigated later.

Fig. 1 shows a comparison of the measured centerline velocity defect w_c with the present calculation. The value of E_{u0} was taken as 1×10^{-5} in the calculation. The result is quite satisfactory and seems to provide the explanation for the rapid deviation from the pure laminar wake solution of Goldstein which is also shown on the same figure for comparison.

Only the results for $x \leq 0.5$ are presented because the three-dimensional effects observed experimentally at larger x are not included in the present formulation. Theoretical calculation for $x > 0.5$ stays practically unchanged near the value of $w_c = .148$. It is also interesting to note that this asymptotic value of w_c corresponds closely to the value where $a_i^* = 0$. At this value a balance exists between various mechanisms responsible for changing the mean flow. We may note that, although it may be somewhat fortuitous, the measured w_c in all the tests has never become smaller than this value before the turbulent region.

Fig. 2 shows the comparison of the measured wake half-width with the one calculated by using Eq. (2.20). The general trend is still satisfactory but not as good as w_c. This disagreement seems to suggest the approximation used in leading to (2.20) may not be appropriate if a better calculation is required. In such cases, the exact relation (2.14) has to be used which includes the contributions from the fluctuation in the momentum integral. An attempt to include

this effect will be discussed in Section 3.5. Also shown on the same plot is the growth of the undisturbed laminar wake. The strong interaction effect induced by the Reynolds stresses is evident from this comparison where the wake width has increased by more than a factor of two.

Fig. 3 gives the theoretically calculated variation of the integrated fluctuation energy, $E_u = \frac{1}{b}\int_0^\infty \overline{u'^2}\, dy$. Since the absolute value of the magnitude of the fluctuating components was not reported by Sato and Kuriki, a direct comparison with the experiment is not possible. However, the variation of the maximum of $(\overline{u_f^2})^{\frac{1}{2}}$ given by Sato-Kuriki on an arbitrary scale shows the similar relative development of the fluctuation. Experimentally, the magnitude of the fundamental mode grows initially according to the exponential law of the linear stability theory but it soon reaches a maximum and then decreases. This fact, which cannot be explained by the linear stability theory alone, may be understood now from the present calculation. However, it should be pointed out that the rapid decrease of E_u does not imply the similar decrease of the total fluctuation energy. This is seen in Fig. 4 where the total integrated fluctuation energy, E_F, is plotted. The variation of E_F is related to the local amplification rate α_i^* given by the linear theory with some correction due to the variation of the mean flow. The rate of change of the total energy starts out in the linear region with a nearly maximum exponential growth and decreases as it moves downstream. The total energy reaches an equilibrium value somewhere near $\alpha_i^* = 0$ when the mean flow ceases to vary, and then slowly decays because of the viscous

dissipating effect. Because of the growth of the wake, a more appropriate measure of the magnitude of the disturbance is the total energy density E_T defined by $E_T = E_F/b$. The variation of E_T is shown in Fig. 5. The reason for the relatively much slower variation of the total fluctuating energy density, E_T, as compared with the sharp decrease in E_u (Fig. 3), is shown in Fig. 6 where the ratio of the integrated energy content in u' to that in v'.

$$k_1/k_2 = \int_0^\infty \overline{u'^2}\, dy^* / \int_0^\infty \overline{v'^2}\, dy^*,$$

is plotted against w_c. The ratio varies by more than a factor of six for the range of w_c encountered here. Therefore, we conclude that the redistribution of the fluctuating energy between the two components u' and v' together with the change of mean flow are responsible for the experimentally observed abnormal phenomena.

The non-dimensional wave propagation velocity, taken as the real part of $c^* = \omega^*/\alpha^*$, measured by Sato-Kuriki, can also be obtained from the present calculation and the comparison is shown in Fig. 7. In view of the scatter of the experimental data, the agreement shown is acceptable. The variation of the wave speed is again a consequence of the changing mean flow.

3.2 Effects of the Initial Values

Although no special attempt has been made in obtaining the theoretical curves discussed in this section to match the experimental data, the arbitrariness in the set of initial values warrants an investigation of their effects. We will study the effects of the two initial values, w_{c0} and E_{u0}, separately in the following.

(A) Effects of w_{c0}

Three cases of variation of w_c corresponding to the initial values of w_{c0} being 0.7, 0.675, and 0.6386, are shown in Fig. 8. The value $w_{c0} = 0.6386$ corresponds to the steady laminar wake solution at $\zeta_0 = .05$ obtained by setting the fluctuation amplitude equal to zero and integrating Eq. (2.15) backward from a far wake solution. The same value of E_{u0} was used for all three curves which give qualitatively the same variation of w_c and asymptote to the same value of w_c. The decrease in w_{c0} results in the decrease in the maximum value of dw_c/dx and in the delay of the onset of non-linear effect. A few experimental data points are also shown there for comparison. It shows that the experimental data agree better with the result of smaller w_{c0} in the region downstream of the maximum slope, but a closer agreement is seen with the larger w_{c0} case for the upstream portion. Fig. 9 gives the variations of the integrated fluctuation energy for the three cases. The general variation is again qualitatively unchanged except for the different locations and levels of the maximum value reached. These differences result from the fact that a higher w_{c0} implies a thinner wake and therefore a higher amplification rate locally.

(B) Effects of E_{u0}

To investigate the effect of E_{u0} on the solutions, a few cases were calculated for $R = 2 \times 10^5$ with the same value of w_{c0} but different E_{u0}. Fig. 10 shows the variations of w_c for three initial values $E_{u0} = 0.1,\ 1.0,\ 3.0 \times 10^{-5}$. The shape of the curves remains practically unchanged. Changing the initial value of E_{u0} amounts

only to a shift of the curve. It is expected from the previous discussions of the physical mechanisms that the magnitude of the disturbance required to cause a sensible deviation of the solution from the undisturbed case is approximately the same over a range of w_c where the laminar viscous term is of the same order. Therefore a smaller initial magnitude of the disturbance will cause the mean flow to follow the laminar solution for a longer distance before the exponentially amplifying disturbance reaches the significant magnitude. This is further illustrated by the variations of the integrated fluctuation energy, E_u, shown on Fig. 11. The shapes are again similar with merely a shift in abscissa. It should be noted that, with the variation of a factor 30 in E_{u0}, the maximum values of E_u are nearly the same and the difference in the "equilibrium" magnitude is negligible. The slight difference in the peak values of E_u is caused by the slight change in the magnitude of the laminar viscous term when the interaction becomes important. In principle, if the initial magnitude of the fluctuation is small enough, the solution approaches the steady laminar wake solution corresponding to $E_{u0} \equiv 0$ which is also shown on Fig. 10 for comparison.

The magnitude of the disturbances existing at the initial stage of the wake depends on many factors which vary from experiment to experiment. These factors include both controllable, e.g., an artificial source of disturbance, and partially controllable, e.g., roughness of the plate, wind tunnel noise level, etc. (If any quantitative calculations are needed, it will be necessary to have some measure of the magnitude of E_{u0}.) This fact is demonstrated by the two sets

of experimental data also shown on Fig. 10. The data points correspond to two different models tested under the same freestream conditions. Model I has a sharp trailing edge but Model II has a blunt one. As expected, a larger E_{u0} will be associated with Model II which shows the right trend as indicated by the calculations.

3.3 Effect of Reynolds Number

Since the inviscid Rayleigh equation has been used to obtain the local solutions for the fluctuation, the integrals, k_i, are universal functions of w_c for all Reynolds number. This may be seen from Eq. (2.19) where the eigenvalue and the corresponding eigenfunction are indicated to be functions of w_c and ω^*. The non-dimensional frequency ω^* is related to the physical angular frequency by

$$\omega^* = \omega b = \frac{bL}{U} \times \text{(physical frequency)} \qquad (3.3)$$

It was found experimentally by Sato and Kuriki that the physical frequency of the most unstable sinusoidal fluctuation observed in the linear region of the wake follows a 3/2 power law as the Reynolds number varies. Furthermore, the half-width, b, is clearly seen from Eq. (2.14) to be varying with the drag coefficient which is proportional to $R^{-\frac{1}{2}}$. Therefore, if we chose to follow the most unstable frequency at various freestream Reynolds numbers, the value of ω^* is a constant which is independent of R. Thus, the same functional relations $k_i(w_c)$ may be used for different Reynolds numbers that greatly simplify the investigation of the effects of Reynolds number.

Fig. 12 shows the variations of w_c for four values of Reynolds numbers. The same set of initial values, $w_{c0} = 0.7$ and $E_{u0} = 1 \times 10^{-5}$ has been used in obtaining the solutions, in order to isolate the effects

of Reynolds number. The effect on the solution is somewhat similar to the effect of changing the initial magnitude of the fluctuation E_{u0}. In fact, it may be seen from Eq. (2.27) that the ratio of the Reynolds stresses term to the laminar viscous term is of the order $|A|^2 \sqrt{R}$. Hence, the effect of R on the beginning of transition is similar to the effect of E_{u0}. However, the effect of R differs through its persistent influence over the whole non-linear region other than a mere shift of the abscissa. When the Reynolds number decreases, the viscous damping term becomes more important in the non-linear region, therefore the overall transition becomes smoother.

Also shown on Fig. 12 are two sets of experimental data of Sato and Kuriki at $R = 2 \times 10^5$, 1×10^5 correspondingly. The agreement in the trend and even the quantitative effect are fairly good considering the fact that if $E_{u0} = 1 \times 10^{-5}$ were correct for the case of $R = 2 \times 10^5$, the same value of E_{u0} might have been too large for the smaller Reynolds number case due to a relatively lower tunnel noise level.

Because of the persistent influence of the Reynolds number on the interaction, its effect on the fluctuation energy is more pronounced than the effect of E_{u0}. The result is shown on Fig. 13 where it may also be noted that the final equilibrium amplitudes reached are different because of the effect of Reynolds number appearing through the viscous dissipating term in Eq. (2.16). This result is also different from the effect of E_{u0} which leaves the final equilibrium amplitude of the fluctuation practically unchanged.

3.4. Effect of the Viscous Dissipation of the Fluctuation

The effect of the viscous dissipation of the fluctuation on the development of the disturbances was studied by simply setting $I_8 \equiv 0$. Comparison is made on Figs. 14 and 15 for the case of $R = 2 \times 10^5$. With identical initial conditions, Fig. 14 shows that the effect of the viscous term in the fluctuation energy equation on the mean flow is quite small as one would expect. Fig. 15 shows that if the viscous dissipation term is absent, a final equilibrium amplitude, namely another laminar oscillatory flow, is reached. However, because of the effect of the viscous dissipation, this equilibrium condition cannot maintain itself and the amplitude decays slowly as it proceeds further downstream to account for the energy loss.

3.5 Effect of Coupling b to w_c

The assumption of neglecting the contribution from the fluctuating components in the integrated momentum equation, which leads to a simple relation (2.20) between b and w_c, is now examined. From the calculated results, it is found that the terms, which have been neglected to arrive at the expression (2.20), are indeed small compared to the remaining terms in the initial stage but increase to about 20 percent of the sum of the remaining terms when the amplitude of the fluctuation reaches a maximum. It is therefore desirable to investigate the effect of using the full integral momentum equation.

An exact formulation will require the computation of the integrals, k_i, as functions of two parameters, b and w_c, since $\omega^* = \omega b$. To simplify the analysis, we assume that the integrals may still be taken as functions of w_c only, but the integral momentum, Eq. (2.14),

is used instead of the approximated Eq. (2.20). Then, the wake half-width b is a function of w_c as well as the amplitude of the fluctuation.

The results of such an integration are shown on Figs. 16 to 18 for the case of $R = 2 \times 10^5$. It is clear that the effect on the mean flow velocity variation is quite small. Since a relatively thinner wake is obtained when b is decoupled from w_c, it affects the variation of the fluctuation energy and the final level approached. The variation of wake half-width b for the two cases are shown on Fig. 18 together with the measured results of Sato and Kuriki. The decoupled result agrees better with the measurements, especially in the "equilibrium" wake width.

4. Concluding Remarks

Based on the comparison of the numerical calculations with the experimental data, the present approach brings out the essential features of the non-linear interaction mechanisms in a laminar wake. The theory shows that the relatively rapid deviation of the mean flow velocity along the wake axis from the prediction for a steady laminar wake and the rapid growth of the wake width observed experimentally in the transition region are the consequences of the non-linear effects induced by the finite amplitude disturbances. The streamwise variation of the magnitude of the fluctuation is in favorable agreement with the relative development observed experimentally. The decrease in magnitude of the fluctuation in the latter stage of the non-linear region, which is abnormal in view of the linear stability theory, is found to be a consequence of the wake growth.

Although the present study of the interaction of a single frequency fluctuation with the mean flow through the Reynolds stresses is able to explain most of the observed phenomena in the experiment of Sato and Kuriki, another important aspect of the non-linear mechanism resulted from the quadratic terms χ_1 and χ_2 in the fluctuation equations (2.4) may not be completely ignored. These terms are responsible for the generation of the higher harmonics and the modification of the lower ones. The appearance of the second harmonic and the rather drastic variation of the distributions of the magnitude and phase of the fundamental mode in the non-linear region of the experiments of Sato and Kuriki calls for the inclusion of such effects which will be reported in a forthcoming paper.

In conclusion, the integral method of solution suggested in this paper provides a means for extending and applying the classical hydrodynamic stability to a real problem. Similar procedure can be applied to flows of inviscid nature and governed by two-dimensional disturbances.

REFERENCES

Gold, H. 1963. Stability of laminar wakes. Ph. D. Thesis, California Institute of Technology.

Goldstein, S. 1933. On the two-dimensional steady flow of a viscous fluid behind a solid body. Part I. Proc. Roy. Soc. A, 142, 545.

Kuwabara, S. 1967. Nonlinear instability of plane Couette flow. Phys. of Fluid. Supplement copy on Boundary Layer and Turbulence, 10:9, Part II, S 115.

Landau, L. 1944. Stability of tangential discontinuity in compressible fluid C. R. (Doklady) Acad. Sci. U. S. S. R. 44, 311.

McKoen, C. H. 1955. On the stability of a laminar wake. ARC CP303.

Meksyn, D. and Stuart, J. T. 1951. Stability of viscous motion between parallel planes for finite disturbances. Proc. Roy. Soc. A, 208, 517.

Sato, H. and Kuriki, K. 1961. The mechanism of transition in the wake of a thin flat plate placed parallel to a uniform flow. J. Fluid Mech. 11, 321.

Stuart, J. T. 1956. On the role of the Reynolds stresses in stability theory. J. Aero. Sci. 23, 86.

Stuart, J. T. 1958. On the non-linear mechanics of hydrodynamic stability. J. Fluid Mech. 4, 1.

Stuart, J. T. 1960. On the non-linear mechanics of wave disturbances in stable and unstable parallel flows. Part 1. The basic behavior in plane Poiseuille flow. J. Fluid Mech. 9, 353.

Taylor, G. I. 1923. Stability of a viscous liquid contained between two rotating cylinders. Phil. Trans. A, 223, 289.

Watson, J. 1960. On the non-linear mechanics of wave disturbances in stable and unstable parallel flows Part 2. The development of a solution for plane Poiseuille flow and for plane Couette flow. J. Fluid Mech. 9, 371.

Watson, J. 1962. On spatially-growing finite disturbances in plane Poiseuille flow. J. Fluid Mech. 14, 211.

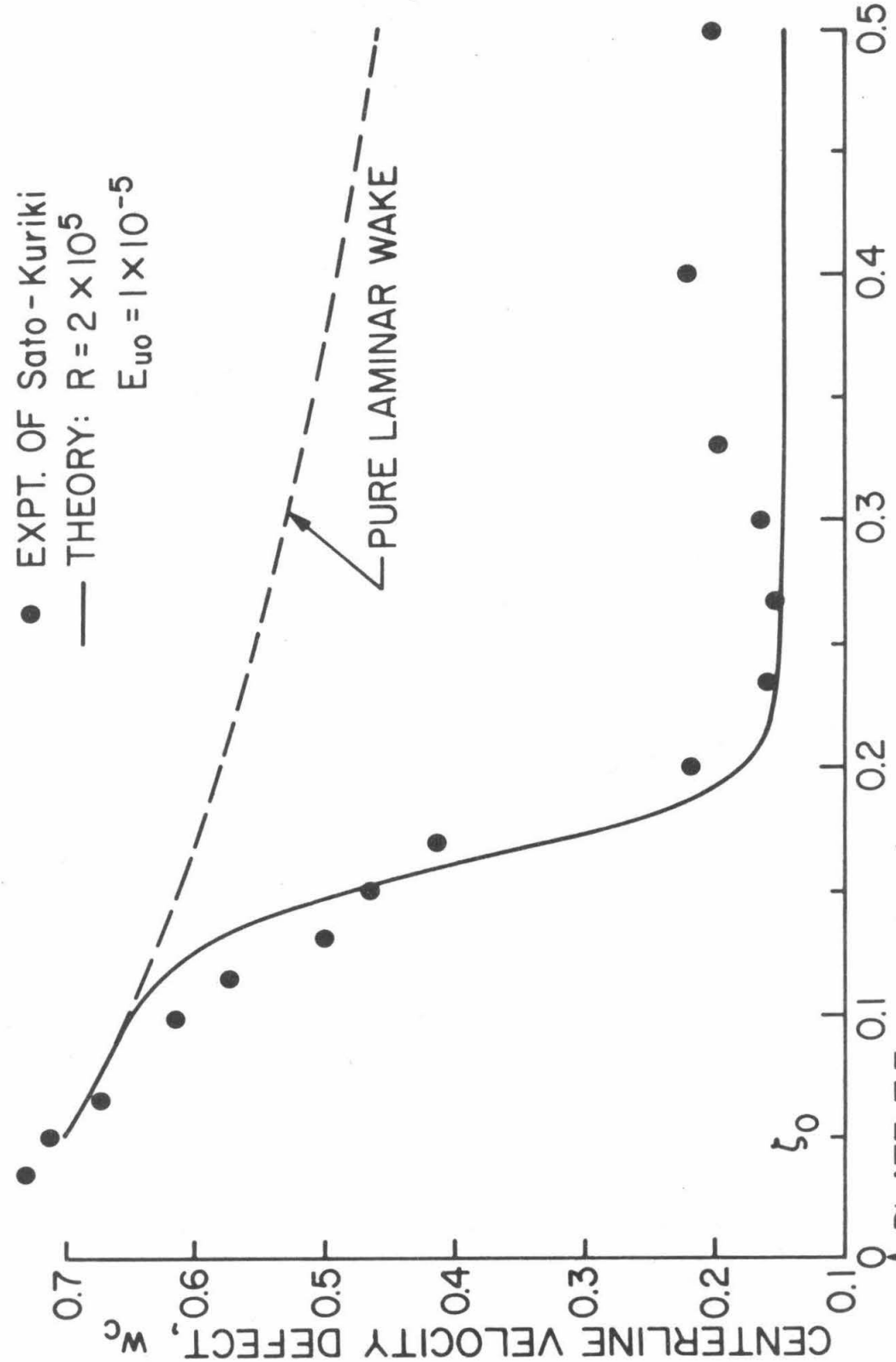

Fig. 1. Comparison of the Mean Centerline Velocity Defect, w_c

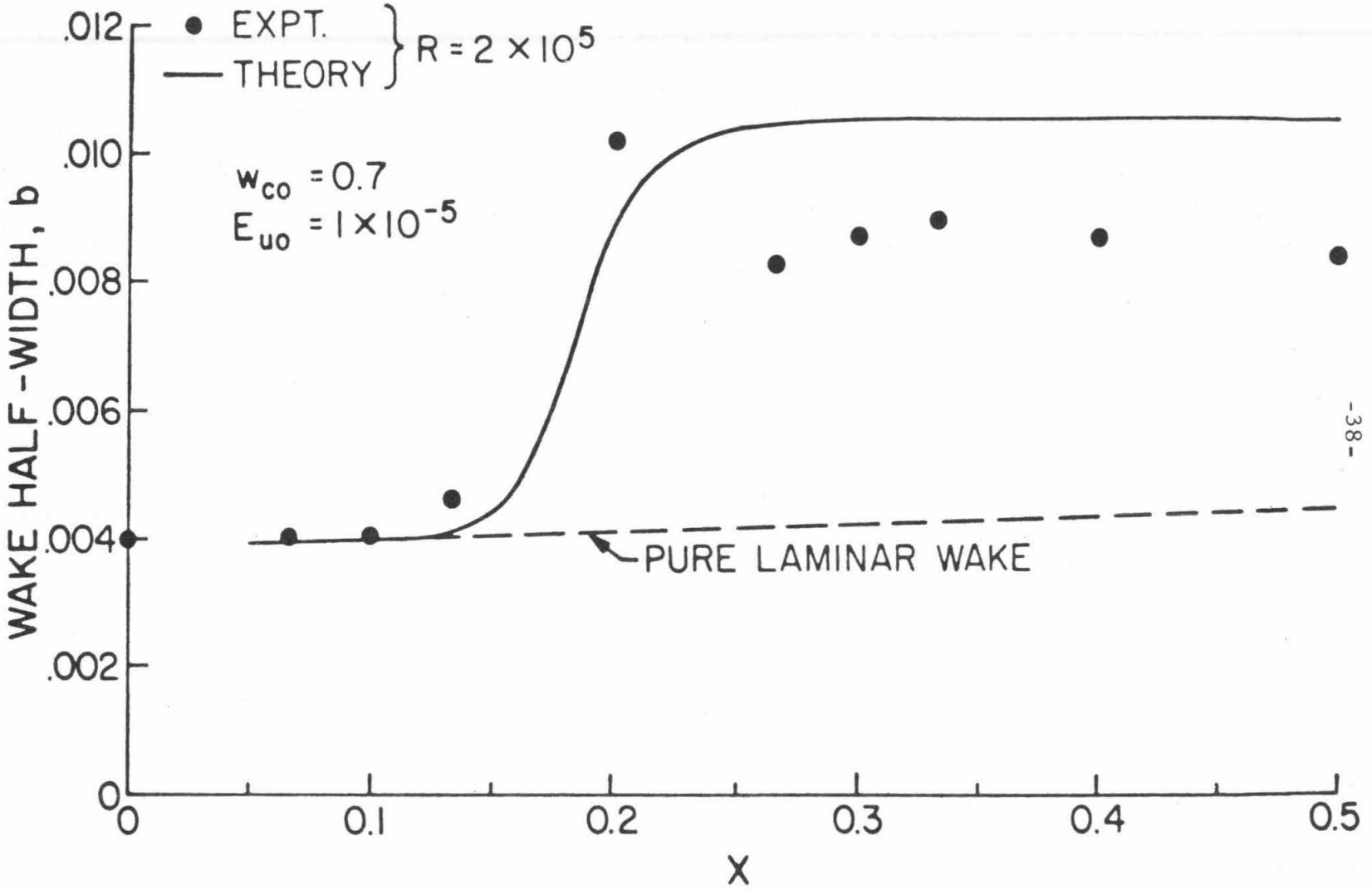

Fig. 2. Comparison of the Wake Half-width b

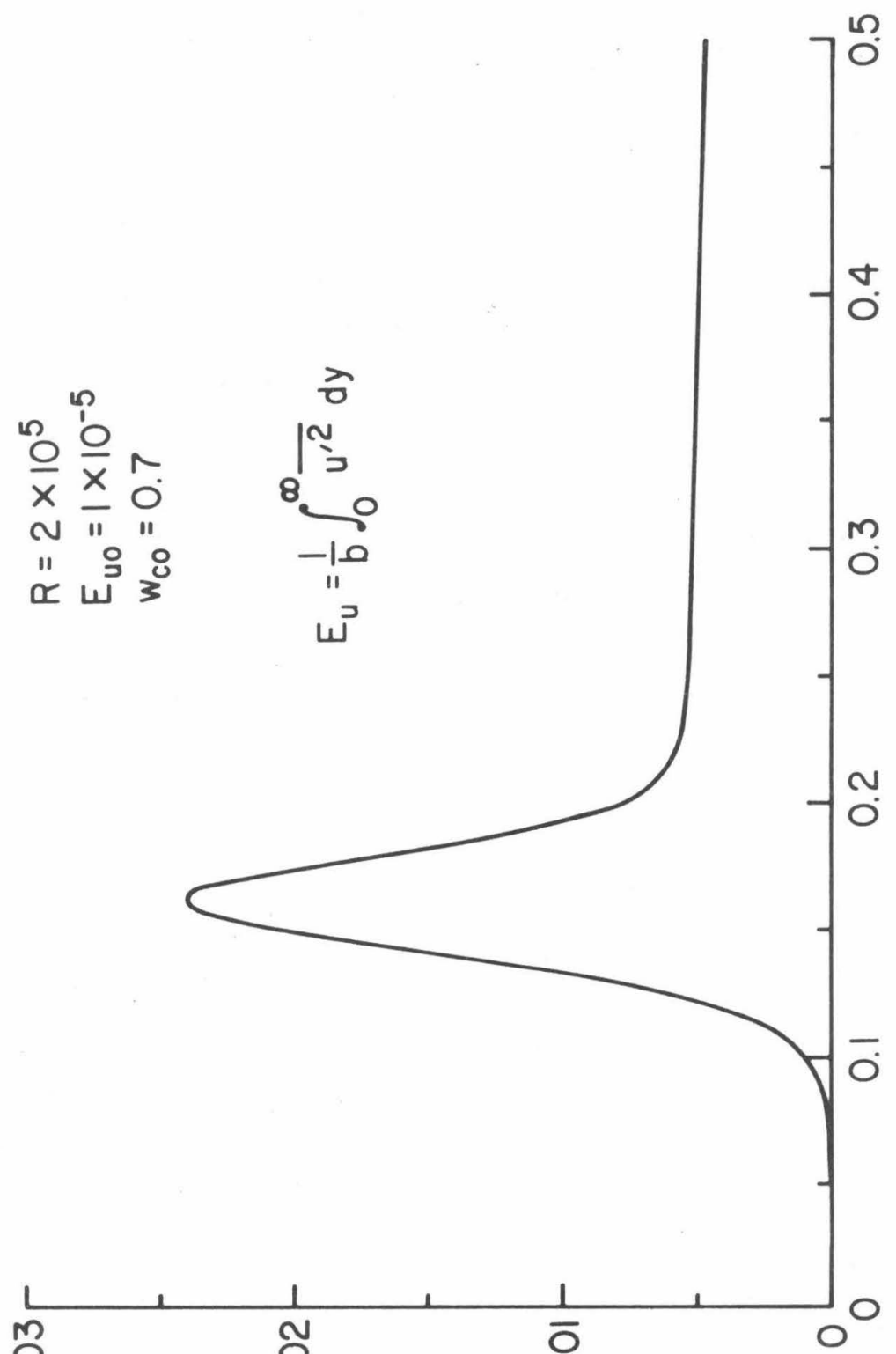

Fig. 3. Calculated Variation of the Integrated Fluctuation Energy in the u'-component E_u

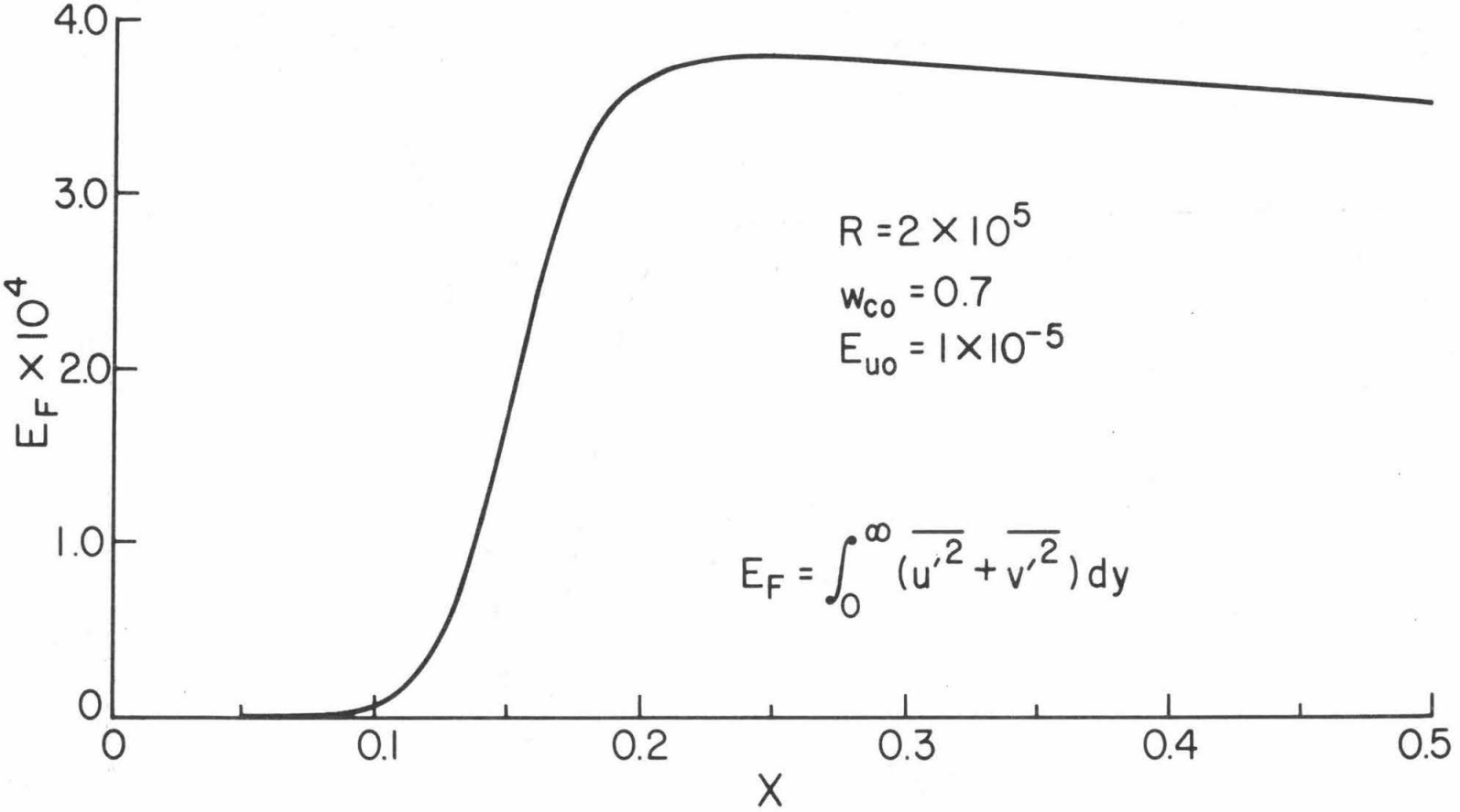

Fig. 4. Variation of the Total Integrated Fluctuation Energy E_F

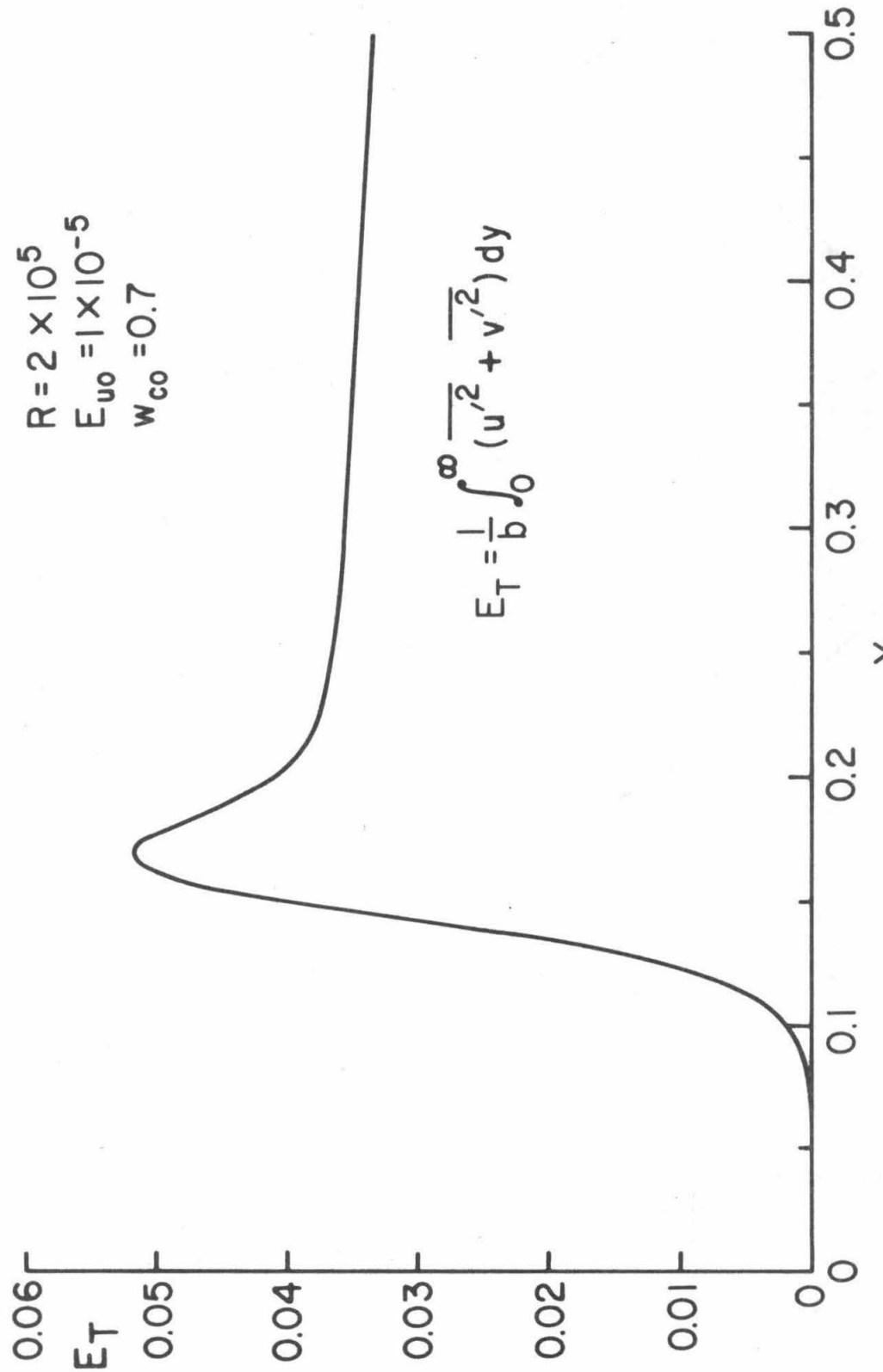

Fig. 5. Variation of the Total Integrated Fluctuation Energy Density E_T

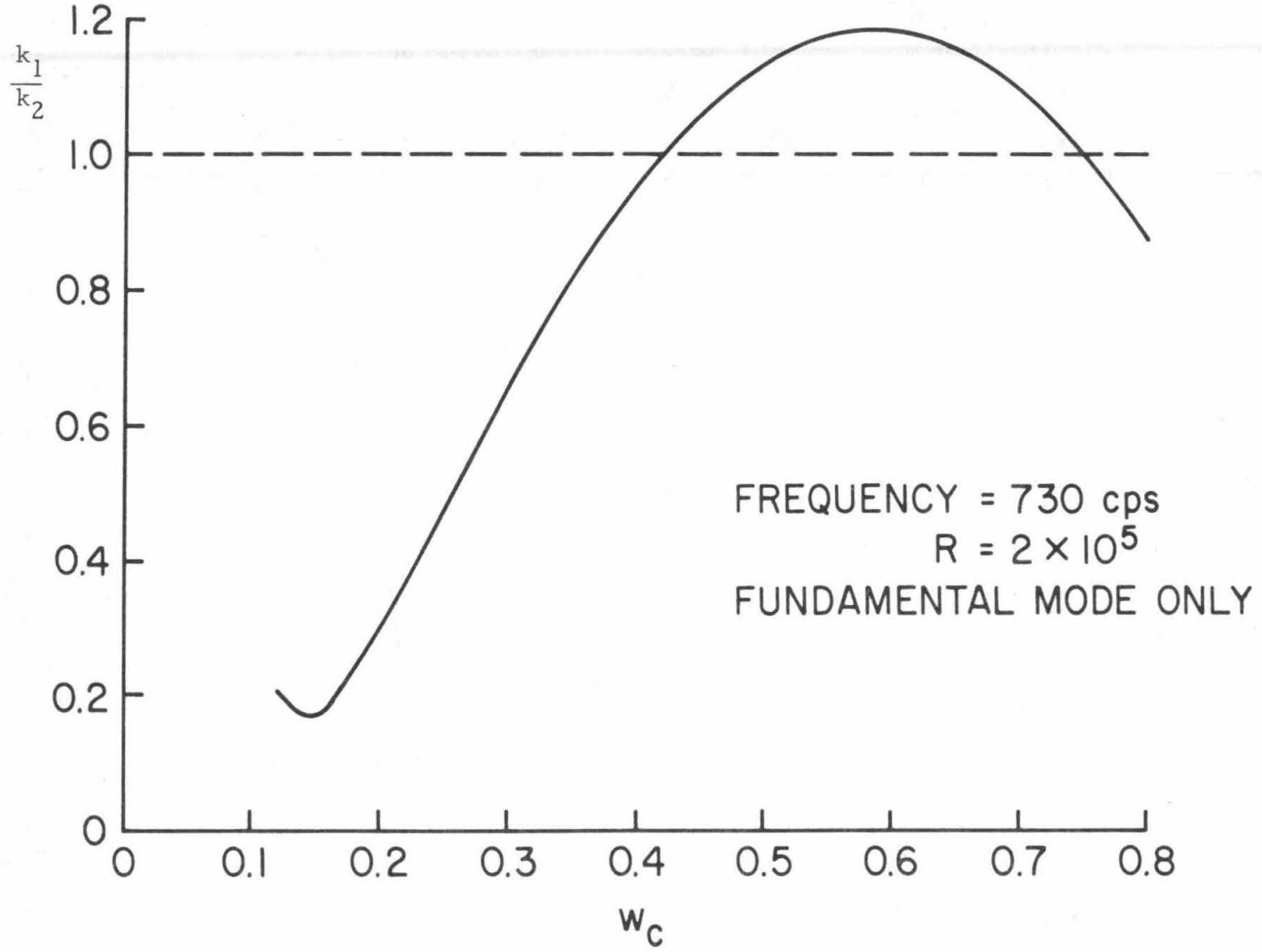

Fig. 6. Relative Energy Content in the u′ and v′ Components as Function of w_c

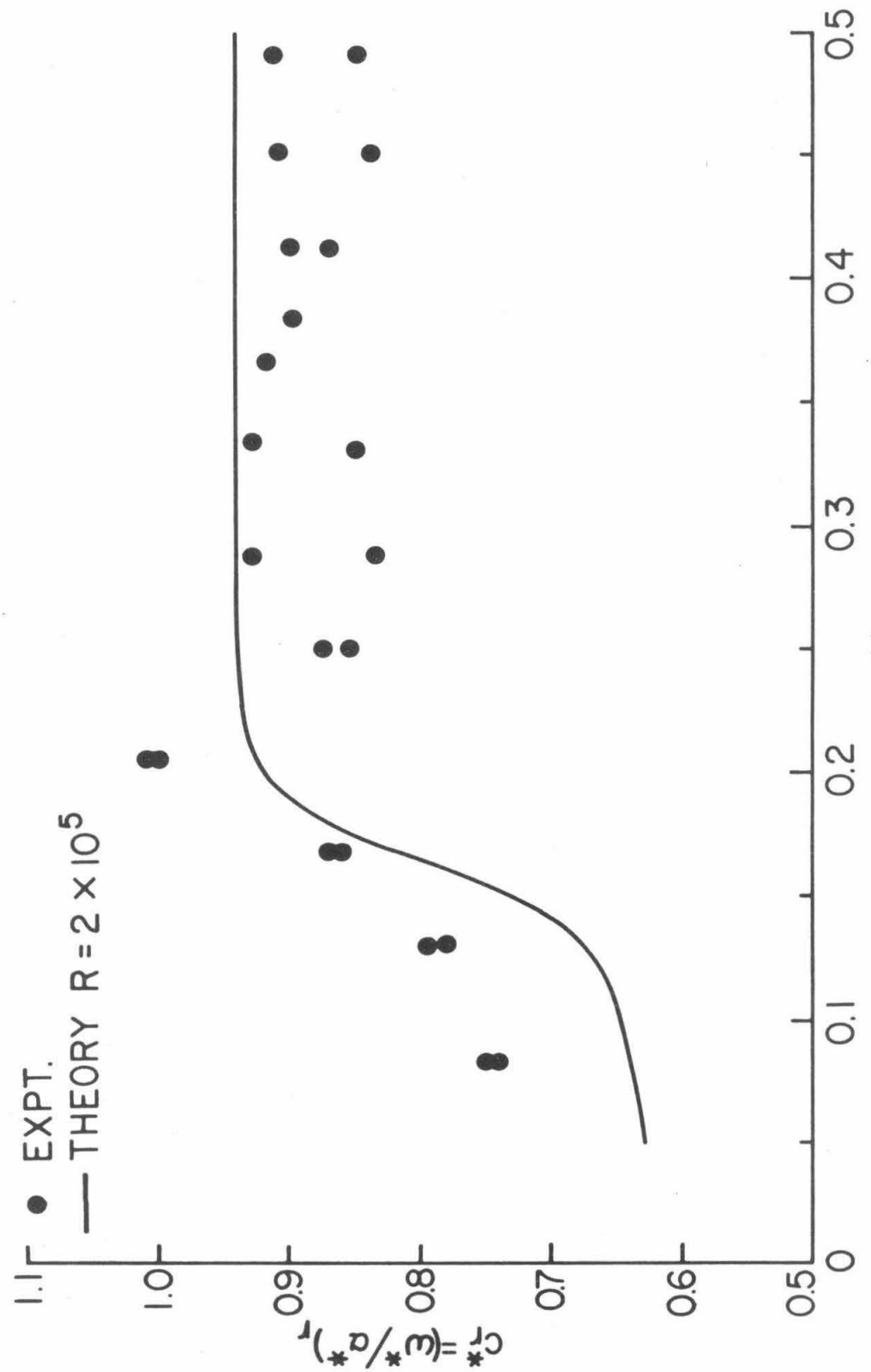

Fig. 7. Comparison of the Non-Dimensional Wave Propagation Velocity c_r^*

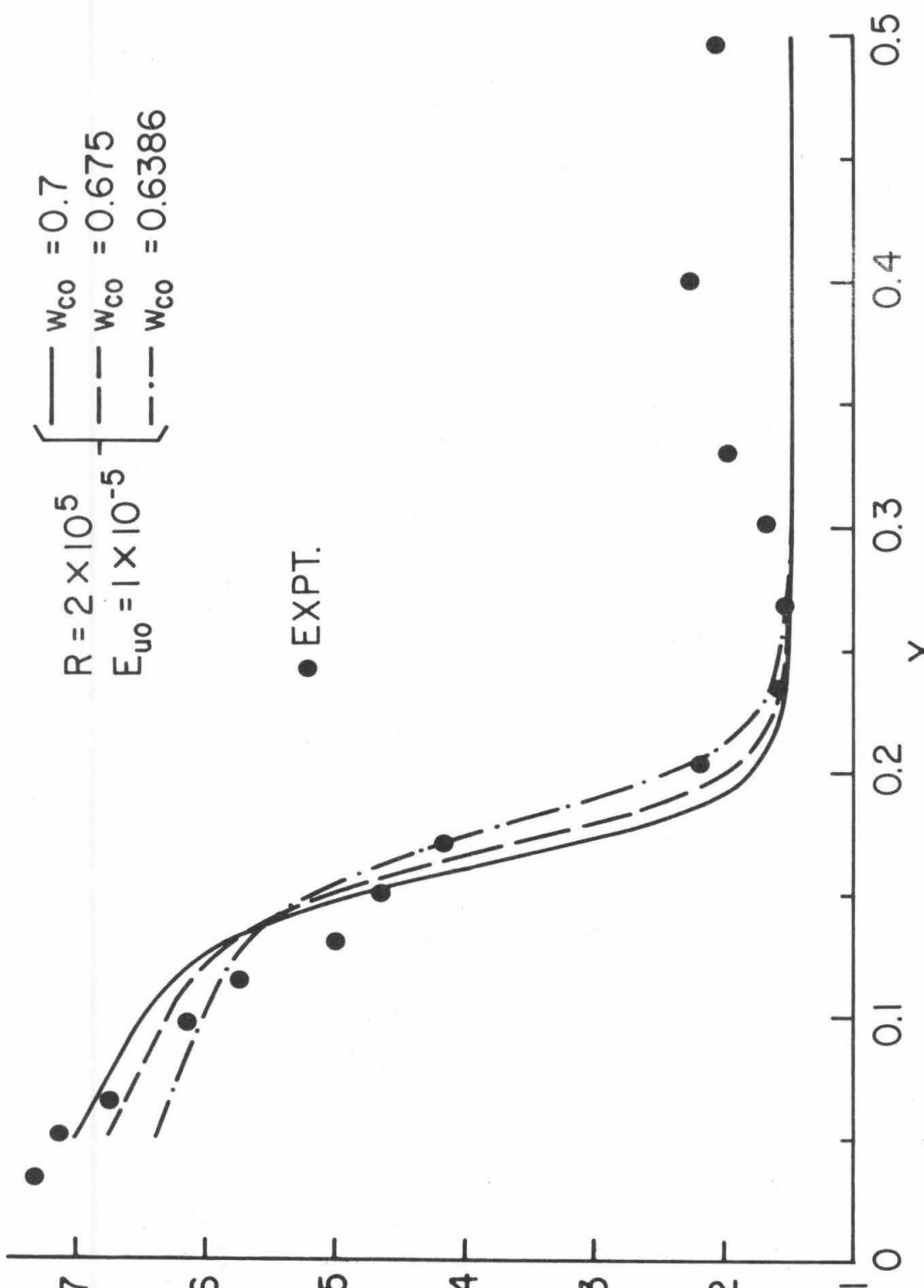

Fig. 8. Effect of $w_{c)}$ on the Variation of w_c

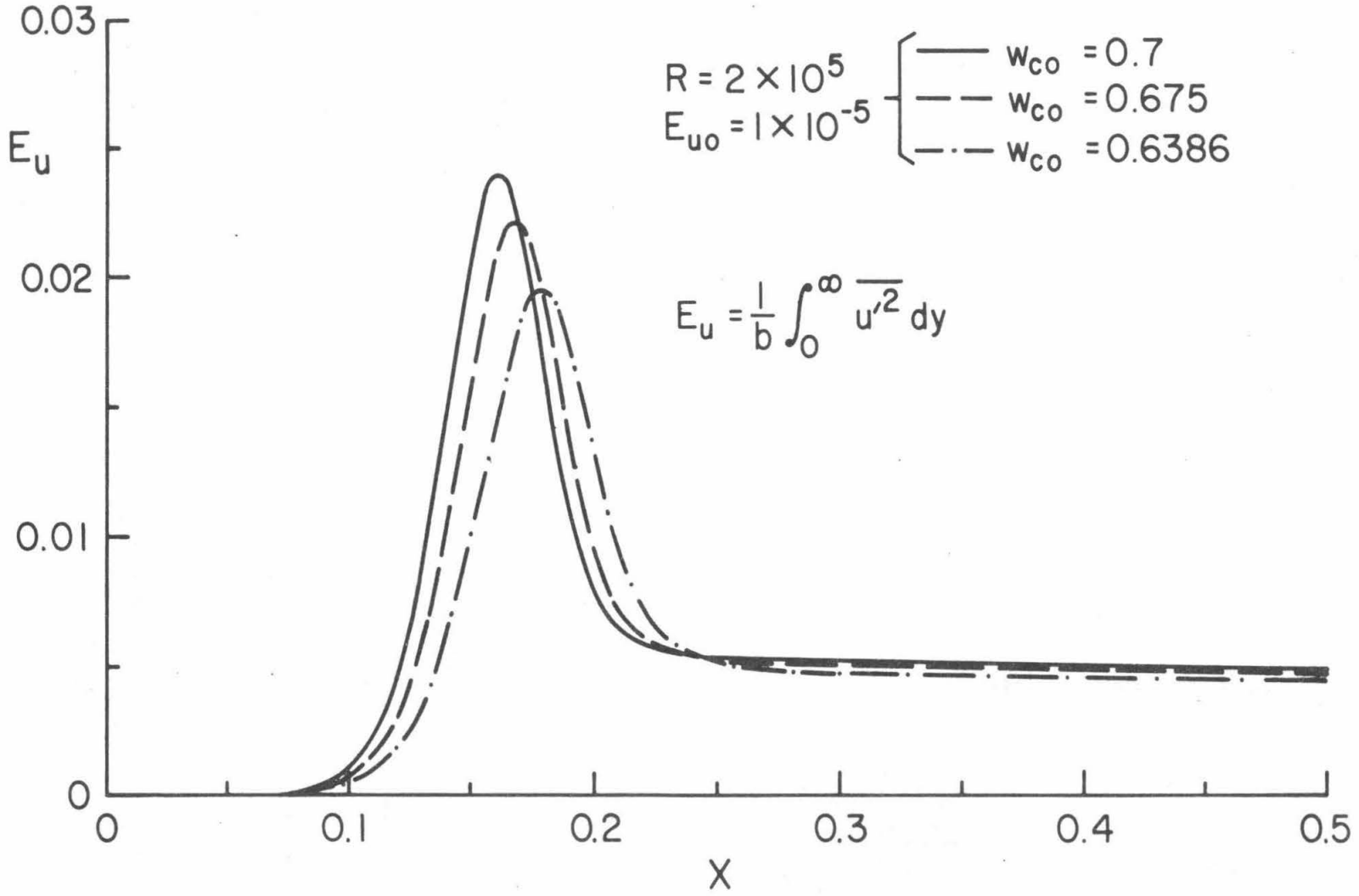

Fig. 9. Effect of w_{c0} on the Variation of E_u

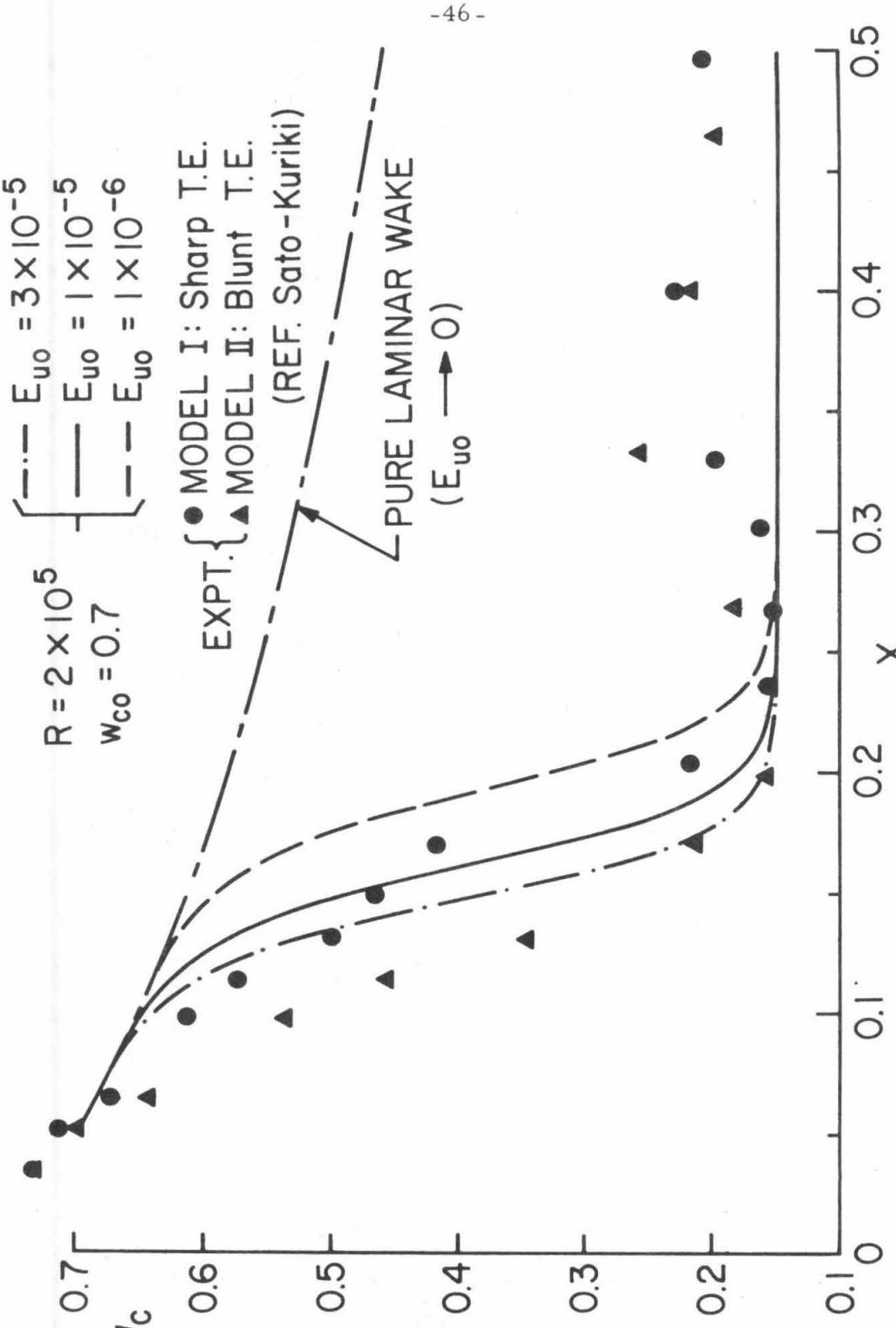

Fig. 10. Effect of E_{u0} on the Variation of w_c

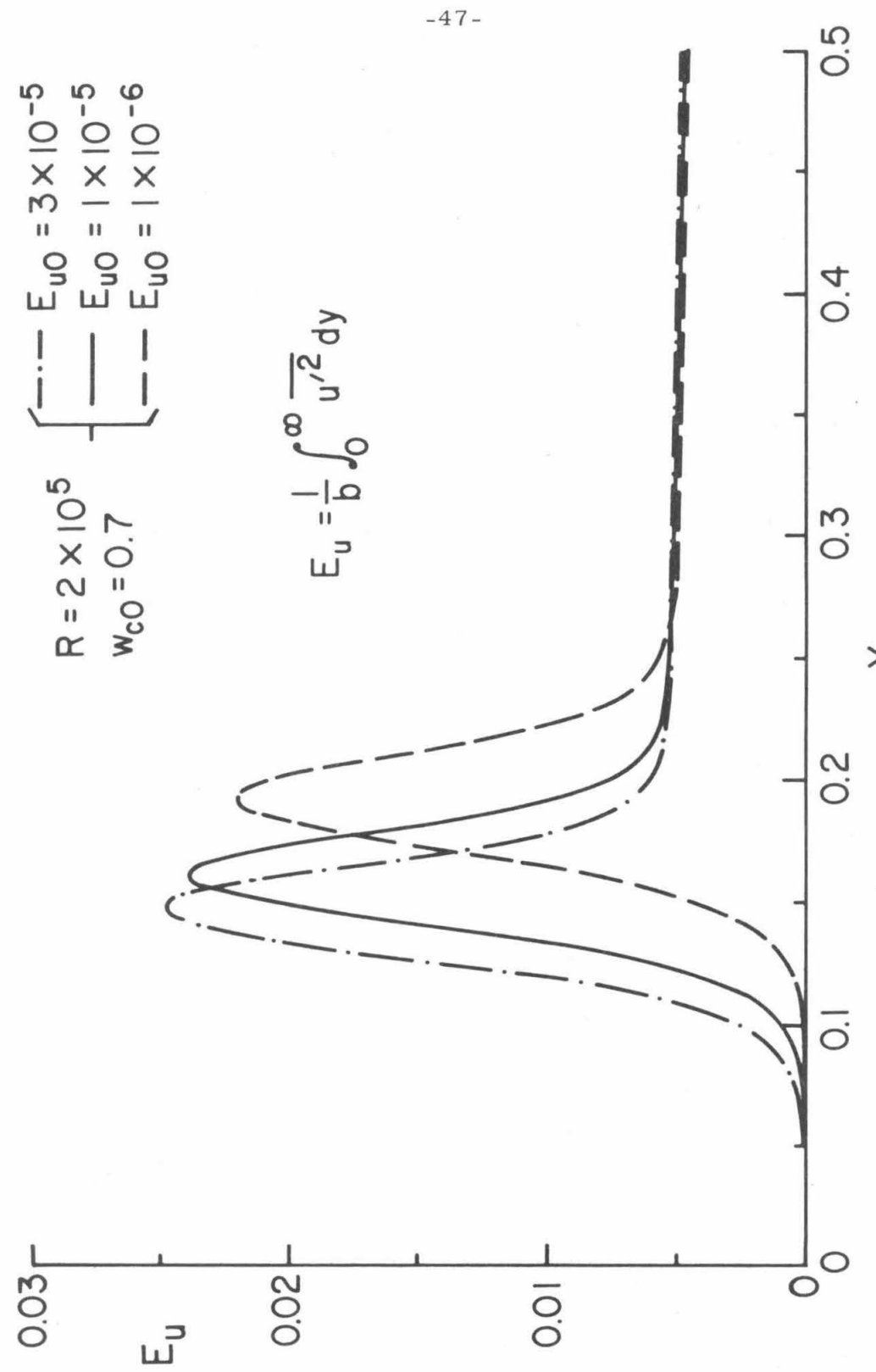

Fig. 11. Effect of E_{u0} on the Variation of E_u

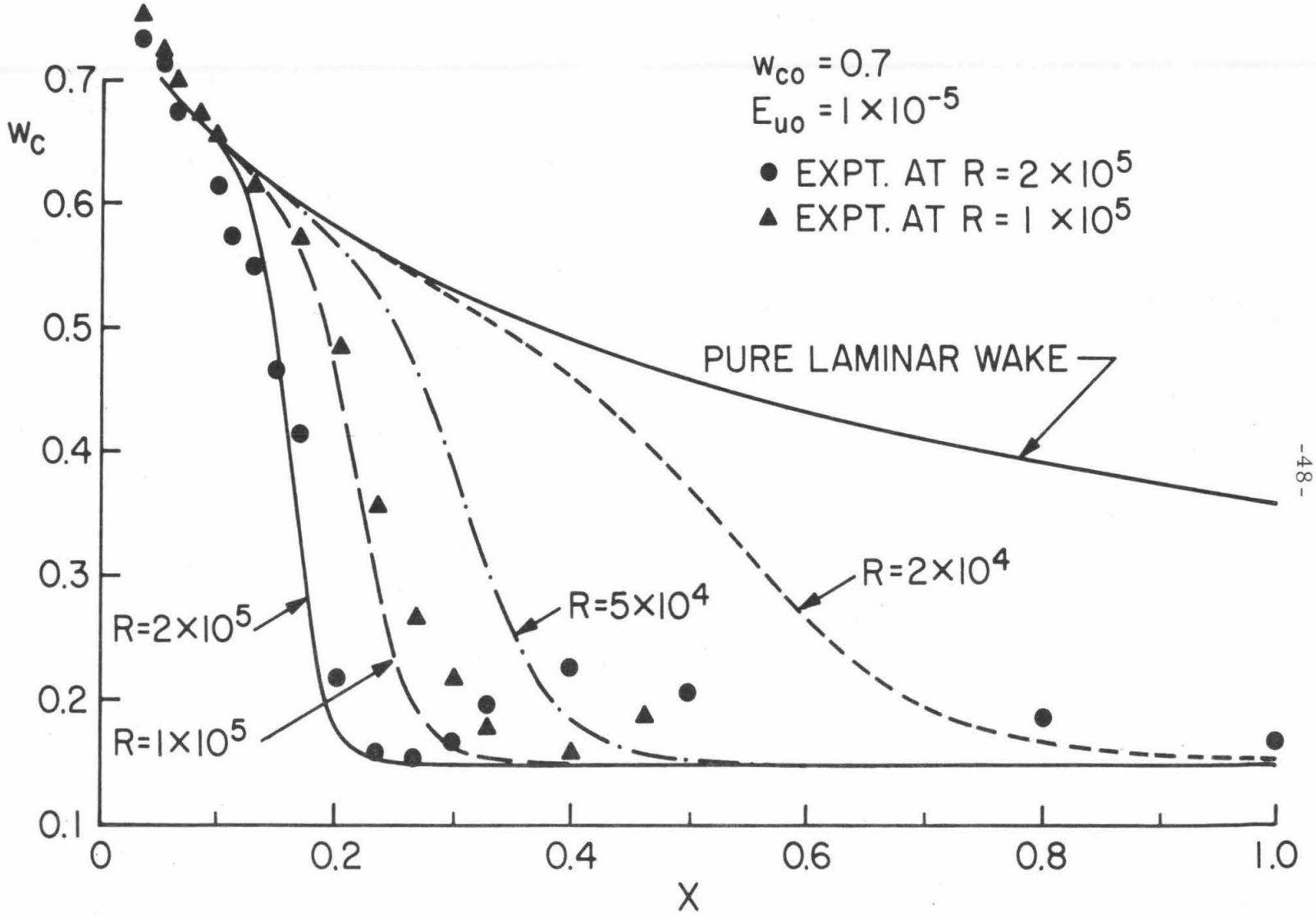

Fig. 12. Reynolds Number Effect on w_c and Comparison with the Experiments

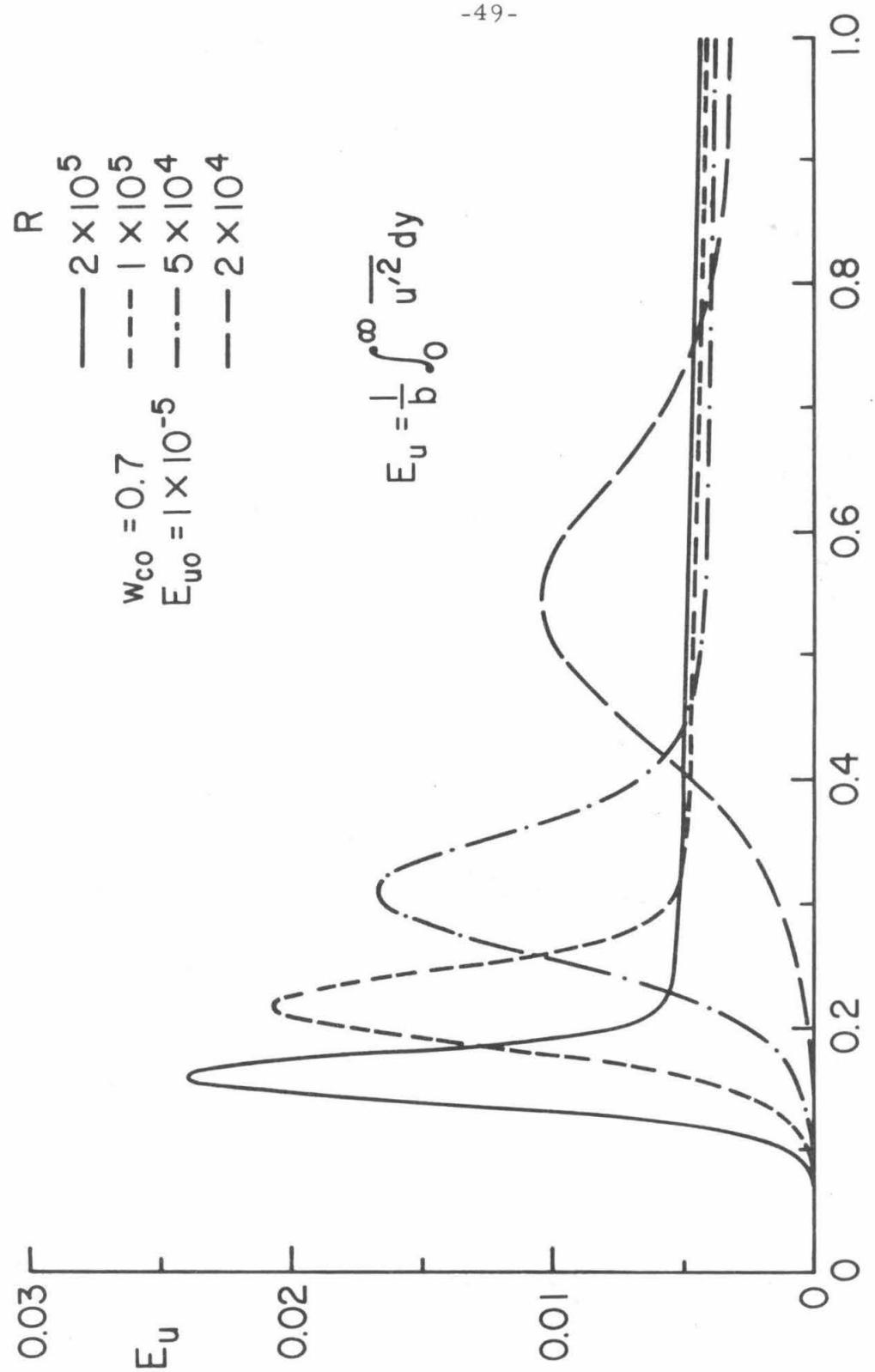

Fig. 1?. Reynolds Number Effect on E_u

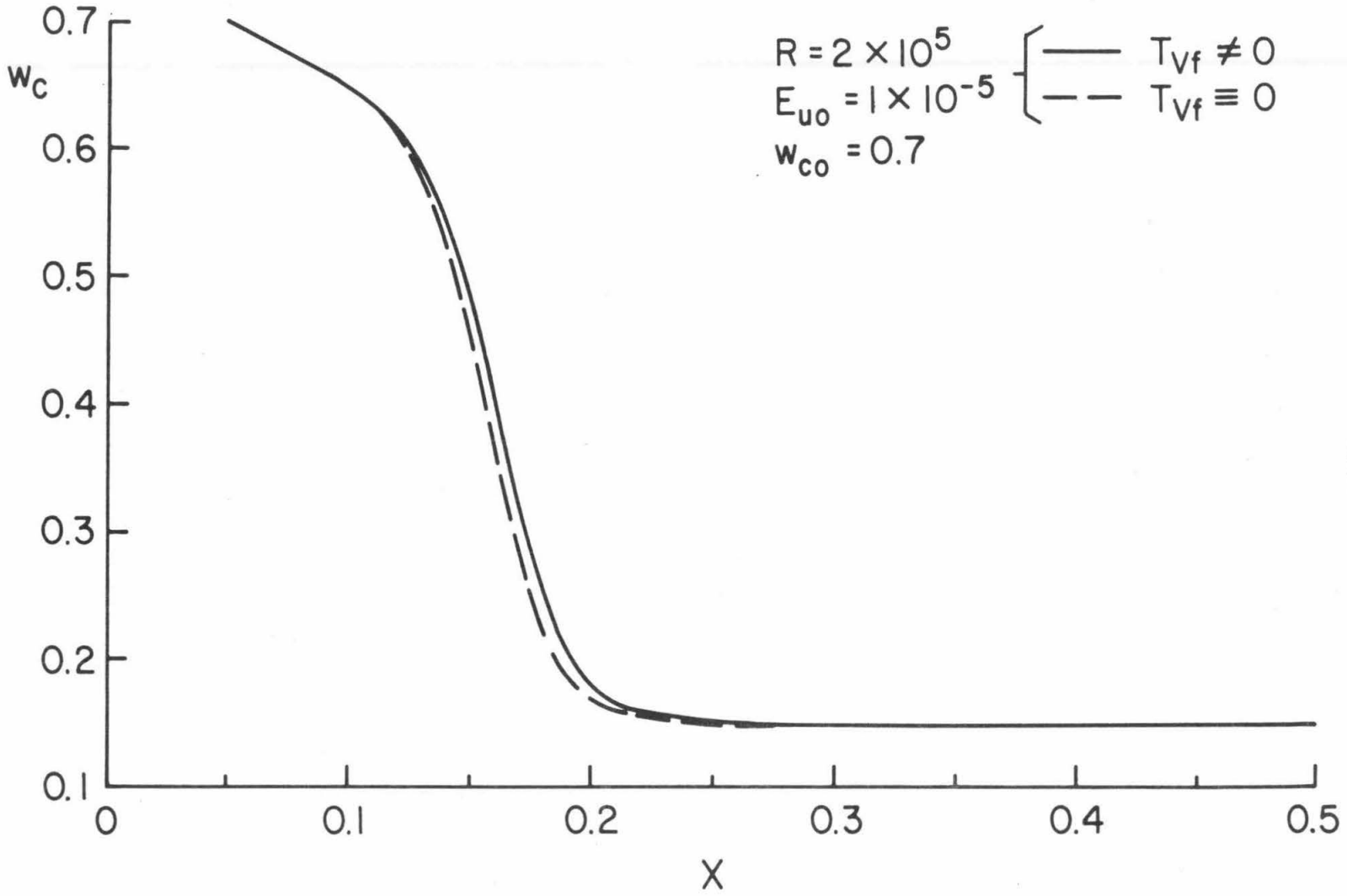

Fig. 14. Effect of the Viscous Dissipation Term T_{vf} on w_c

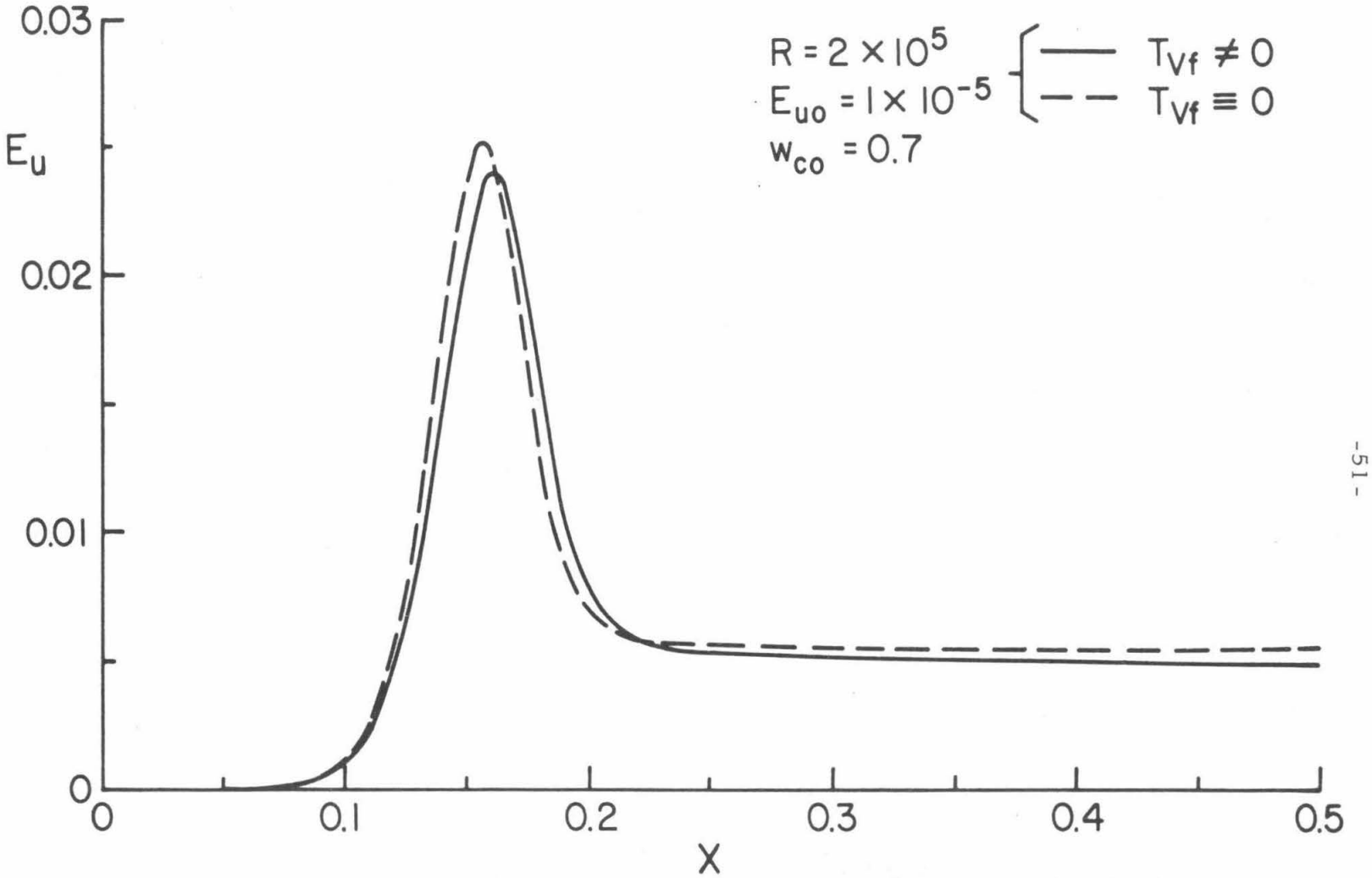

Fig. 15. Effect of the Viscous Dissipation Term T_{vf} on E_u

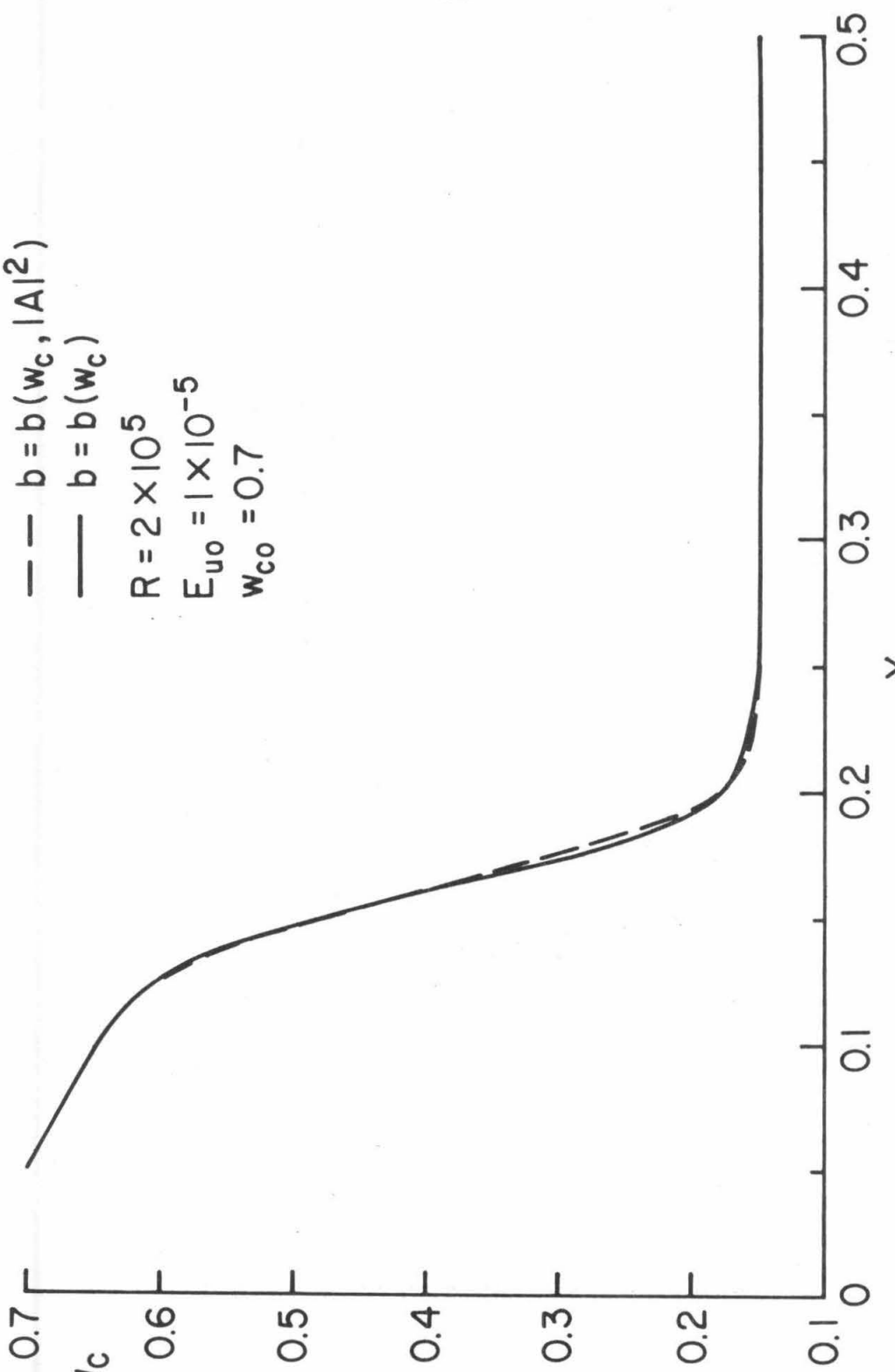

Fig. 16. Effect of Decoupling b from w_c on the Variation of w_c

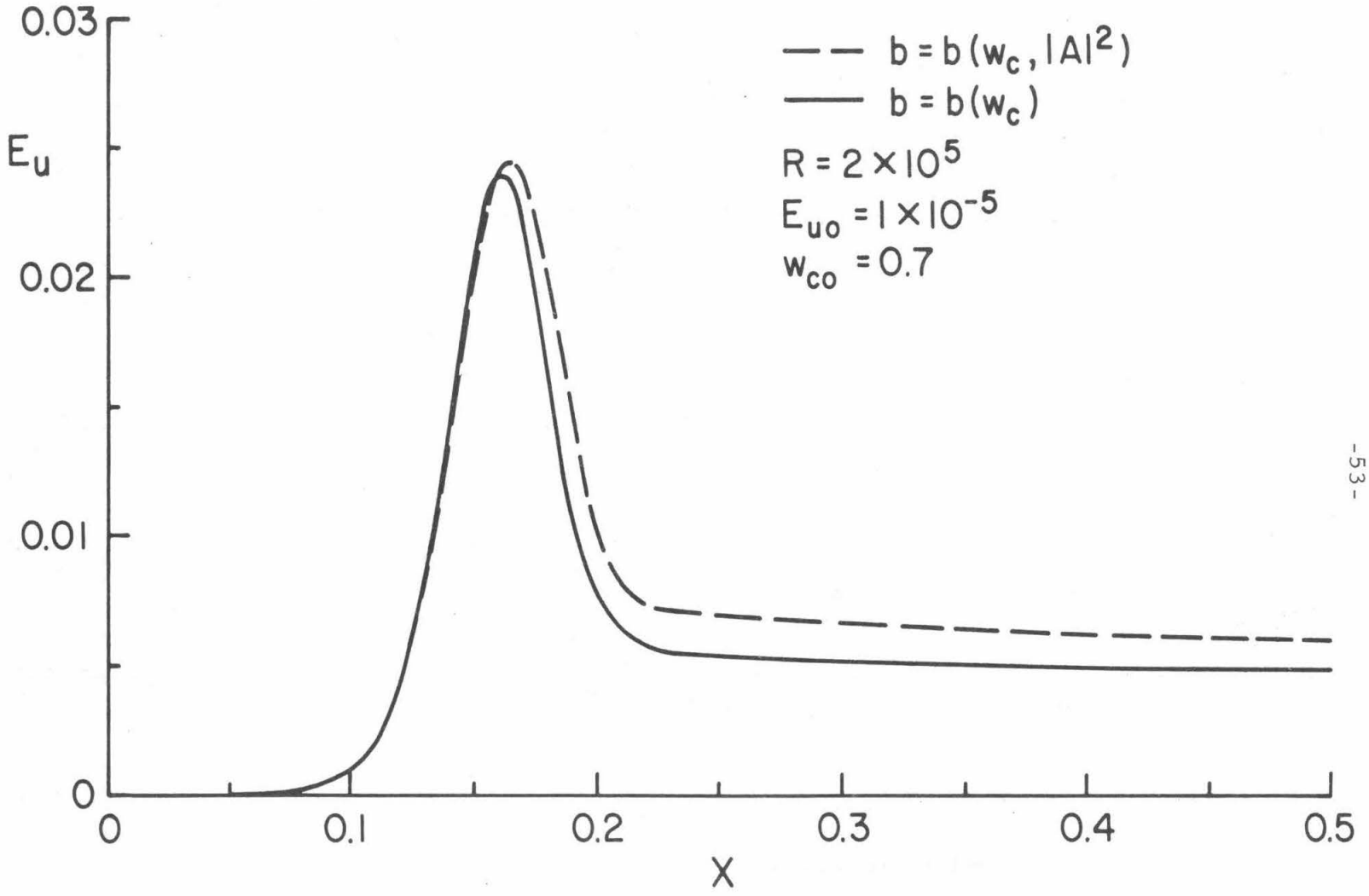

Fig. 17. Effect of Decoupling b from w_c on the variation of E_u

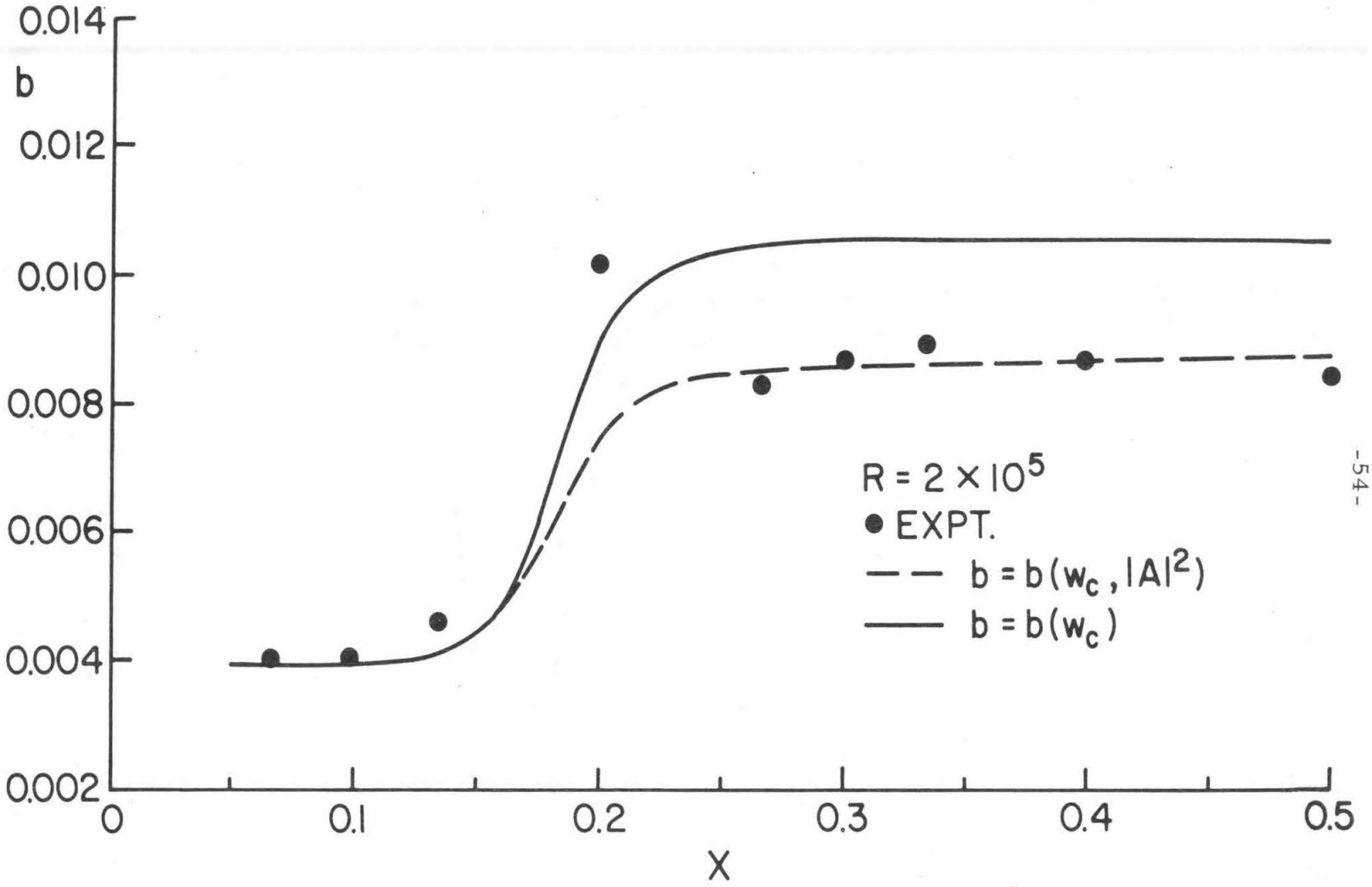

Fig. 18. Comparison of Wake Half-Width for $b=b(w_c)$ and $b=b(w_c, |A|^2)$

DISTRIBUTION LIST

United States Army

U. S. Army Research Office (Durham)
Box CM, Duke Station
Durham, North Carolina 27706
Attention: Information Processing Office
(30 copies)
Attention: Mr. James J. Murray

Office of the Secretary of Defense
Advanced Research Projects Agency
Washington, D. C. 20301
Attention: Mr. Kent Kresa, Program Mgr.
Applied Gas Dynamics Research

Redstone Scientific Information Center
U. S. Army Missile Command
Redstone Arsenal, Alabama - 35809
Attention: Chief, Document Section

U. S. Army Ballistic Research Laboratories
Exterior Ballistics Laboratory
Aberdeen Proving Ground, Maryland - 21005
Attention: Dr. F. D. Bennett, Chief
Attention: Dr. Raymond Sedney

United States Air Force

AEDC (ARO, Inc.)
Arnold Air Force Station
Tennessee - 37389
Attention: Library
Attention: Dr. B. H. Goethert
Director of Engineering
Attention: Mr. J. Leith Potter/VKF
Manager, Research Branch

Aeronautical Research Laboratories
Building 450
Wright-Patterson AFB, Ohio - 45433
Attention: ARR (Mr. Fred L. Daum)
Attention: ARR (Mr. A. W. Fiore)
Attention: ARD-2 (Dr. Roscoe H. Mills)
Scientific Advisor (Aeromechanics)
Attention: ARR (Dr. Robert Korkegi

Dr. Alexander H. Flax
Asst. Secretary of the Air Force
Research and Development
Room 4E 968
Pentagon Building
Washington, D. C. 20330

Office of Research Analyses, OAR
Holloman Air Force Base
New Mexico - 88330
Attention: RRR (Dr. Gerhard R. Eber)

APGC (PGAPI)
Eglin Air Force Base
Florida - 32542

Air Force Office of Scientific Research
(SREM)
Building T-D
Washington, D. C. 20301
Attention: Milton Rogers

U. S. Air Force Inst. of Technology
Library
AFIT-LIB, Bldg. 640, Area B.
Wright-Patterson AFB, Ohio 45433

Armed Services Technical
Information Agency
Air Research and Development Command
United States Air Force
Arlington Hall Station
Arlington, Virginia 22212
Attention: ASTIA (TIPCA)
10 copies

RTD
Wright Patterson AFB, Ohio - 45433
Attention: FDMG (Richard R. Smith)

NASA

NASA
Ames Research Center
Moffett Field, California 94035
Attention: Library

NASA
Langley Research Center
Langley Station
Hampton, Virginia - 23365
Attention: Librarian
Attention: Mr. Eugene S. Love,
Assistant Chief
Aero-Physics Division
Building 1236
Attention: Mr. Charles H. McLellan,
Head, Mission Analysis Group
Building 1220

NASA
George C. Marshall Space Flight Center
Huntsville, Alabama - 35812
Attention: Aero-Astrodynamics Laboratory
M-Aero-TS
3 copies
Attention: M-Aero-A
Mr. Werner K. Dahm

NASA
Lewis Research Center
21000 Brookpart Road
Cleveland, Ohio 44134
Attention: Library

Scientific and Technical Information Facility
P. O. Box 5700
Bethesda, Maryland 20014
Attention: NASA Representative (S-AK/DL)

Miscellaneous Government Agencies

Batelle Memorial Institute
505 King Avenue
Columbus, Ohio 43201
Attention: Batelle-DEFENDER

Canadian Joint Staff
Defence Research Member
2450 Massachusetts Avenue, N. W.
Washington, D. C. 20008

European Office, OAR
Technical Information Office
APO 667
New York, N. Y. 10001

Navy Department
U. S. Naval Research Laboratory
Washington, D. C. - 20390
Attention: Director

U. S. Department of Commerce
National Bureau of Standards
Washington, D. C. - 20234
Attention: Dr. G. B. Schubauer
Chief, Fluid Mechanics Section

Universities

Brown University
Providence, R. K. 02912
Attention: Dr. J. T. C. Liu
Division of Engineering
Attention: Professor R. E. Meyer
Div. of Applied Mathematics
Attention: Professor M. Sibulkin
College of Engineering

The President's Office
Carnegie Institute of Technology
Pittsburgh, Pennsylvania 15213
Attention: Dr. H. Guyford Stever

Case Institute of Technology
University Circle
Cleveland, Ohio 44106
Attention: Dr. G. Kuerti
Dept. of Mech. Engrg.
Attention: Dr. Eli Reshotko
Division of Engineering

University of California
Department of Engineering
Los Angeles, California 90024
Attention: Professor A. F. Charwat
Attention: Dr. C. Y. Liu
Attention: Dr. N. Rott

University of California, San Diego
Dept. of Aerospace and Mechanical
Engineering Sciences
P. O. Box 109
La Jolla, California 92037
Attention: Dr. Paul A. Libby

University of Colorado
Joint Institute of Laboratory Astrophysics
1511 University Avenue
Boulder, Colorado 80302
Attention: Dr. W. W. Willmarth

Columbia University
Department of Mechanical Engineering
New York, N. Y. 10027
Attention: Professor Robert A. Gross

Cornell University
Graduate School of Aerospace Engineering
Ithaca, New York 14850
Attention: Library
Attention: Dr. William R. Sears
Attention: Professor S. F. Shen

University of Florida
Department of Aerospace Engineering
Gainesville, Florida 32601
Attention: Professor David T. Williams

Georgia Institute of Technology
School of Aerospace Engineering
225 North Avenue
Atlanta, Georgia 30332
Attention: Dr. Howard McMahon

Harvard University
Division of Engineering and Applied Physics
Cambridge, Massachusetts 02138
Attention: Dr. Howard W. Emmons

The Johns Hopkins University
Department of Mechanics
Baltimore, Maryland - 21218
Attention: Dr. Francis H. Clauser
Attention: Dr. Stanley Corrsin

The Johns Hopkins University
Applied Physics Laboratory
8621 Georgia Avenue
Silver Spring, Maryland 20910
Attention: Dr. L. L. Cronvich
Attention: Dr. F. K. Hill

The Johns Hopkins University
Aeronautics Building
Baltimore, Maryland - 21218
Attention: Professor L. S. G. Kovasznay

University of Illinois
Department of Aeronautical and
Astronautical Engineering
101 Transportation Building
Urbana, Illinois 60680
Attention: Professor Harold O. Barthel
Attention: Dr. Allen I. Ormsbee

Illinois Institute of Technology
Dept. of Mechanical and Aerospace Engrg.
Chicago, Illinois 60616
Attention: Professor Mark V. Morkovin

Lehigh University
Department of Physics
Bethlehem, Pennsylvania 18016
Attention: Dr. Raymond J. Emrich

University of Maryland
Institute for Fluid Dynamics and
Applied Mathematics
College Park, Maryland 20201
Attention: Professor J. M. Burgers
Attention: Professor S. I. Pai

Massachusetts Institute of Technology
Department of Aeronautics and Astronautics
Cambridge, Massachusetts 02139
Attention: Dr. C. Forbes Dewey
Room 3-246
Attention: Dr. Morton Finston
Aerophysics Laboratory
Attention: Prof. E. Mollo-Christensen
Room 33-320
Attention: Dr. Ronald F. Probstein
Room 3-254
Attention: Dr. A. H. Shapiro
Room 3-264

University of Michigan
Institute of Science and Technology
BAMIRAC
P. O. Box 618
Ann Arbor, Michigan 48107
Attention: Library
Attention: N. L. Johnson
Attention: Professor V. C. Liu

University of Michigan
Ann Arbor, Michigan - 48104
Attention: Engineering Library

University of Michigan
Department of Aeronautical and
Astronautical Engineering
Ann Arbor, Michigan - 48104
Attention: Dr. Arnold M. Kuethe

University of Michigan
Aeronautical Engineering Laboratories
North Campus
Ann Arbor, Michigan 48105
Attention: Mr. James L. Amick
Aerodynamics Laboratory
Attention: Professor J. A. Nicholls
Aircraft Propulsion Laboratory

University of Minnesota
Institute of Technology
Aero Hypersonic Laboratory
Rosemount, Minnesota 55455

New York University
Courant Institute
4 Washington Place
New York, N. Y. 10003
Attention: Library

New York University
School of Engineering and Science
Dept. of Aeronautics and Astronautics
Bronx, New York 10453
Attention: Dr. Antonio Ferri

North Carolina State College
Department of Mechanical Engineering
Raleigh, North Carolina 27607
Attention: Professor R. M. Pinkerton

Northwestern University
Department of Mechanical Engineering
and Astronautical Sciences
The Technological Institute
Evanston, Illinois 60201
Attention: Dr. Ali Bulent Cambel

The Ohio State University
Department of Aeronautical and
Astronautical Engineering
2036 Neil Avenue
Columbus, Ohio 43210
Attention: Mr. Larry X. Besant
Librarian
Attention: Dr. Ting Y. Li
Attention: Prof. Garvin L. Von Eschen

Polytechnic Institute of Brooklyn
Aerospace Institute
527 Atlantic Avenue
Freeport, New York 11217
Attention: Library

Polytechnic Institute of Brooklyn
Graduate Center
Route 110
Farmingdale, New York 11735
Attention: Professor Martin H. Bloom

Princeton University
James Forrestal Research Center
Gas Dynamics Laboratory
Princeton, New Jersey 08540
Attention: Library
Attention: Dr. George Bienkowski
Attention: Prof. Martin H. Bloom
Attention: Prof. S. M. Bogdonoff
Attention: Dr. Luigi Crocco
Attention: Prof. Sin-I Cheng

Purdue University
School of Aeronautical Engineering
West Lafayette, Indiana - 47907
Attention: Aeronautical and Engineering
Sciences Library

Rensselaer Polytechnic Institute
Dept. of Aeronautical Engineering
and Astronautics
Troy, New York - 12181
Attention: Library - Reports Section
Attention: Dr. Herbert S. Glick

University of Rochester
College of Engineering
Department of Mechanical Engineering
River Campus Station
Rochester, New York 14627
Attention: Professor Martin Lessen

Stanford University
Dept. of Aeronautics and Astronautics
Stanford, California - 94305
Attention: Dr. Milton Van Dyke
Attention: Professor Walter G. Vincenti

State University of New York at Buffalo
Engineering Library
Parker Hall
Chemistry Road
Buffalo, New York 14214
Attention: Mrs. Esther Roberts
Engineering Library

University of Southern California
Aerospace School of Engineering
University Park
Los Angeles, California 90007
Attention: Dr. R. E. Kaplan
Attention: Dr. John Laufer
Attention: Dr. H. T. Yang

University of Tennessee
Space Institute
Tullahoma, Tennessee 37388
Attention: Dr. Susan Wu

University of Texas
Defense Research Laboratory
P. O. Box 8029
Austin, Texas - 78712
Attention: Dr. M. J. Thompson

University of Washington
Department of Aeronautics
Guggenheim Hall
Seattle, Washington - 98105
Attention: Professor R. E. Street

Virginia Polytechnic Institute
College of Engineering
Blacksburg, Virginia 24061
Attention: Dr. J. Lukasiewicz

Industrial Research Companies

Aeronautical Research Associates
of Princeton, Inc.
50 Washington Road
Princeton, New Jersey - 08549
Attention: Dr. Coleman du P. Donaldson

Aeronutronics, Division of Philco
Fluid Mechanics Research, ATC
Newport Beach, California 92660
Attention: Dr. Anthony Demetriades
Room 22
Attention: Mr. Dick Spongberg

Aerospace Corporation
P. O. Box 95085
Los Angeles, California 90045
Attention: Dr. J. Logan, Director
Attention: Dr. H. Mirels

AVCO
Research and Advanced Development
Division
201 Lowell Street
Wilmington, Massachusetts 01887
Attention: Dr. Harris Gold
Attention: Mr. P. Levine
Attention: Dr. Barry L. Reeves

Avco-Everett Research Laboratory
2385 Revere Beach Parkway
Everett, Massachusetts 02149
Attention: Library

Bell Telephone Laboratories, Inc.
Analytical Mechanics Dept.
Whippany, New Jersey 08981
Attention: Dr. P. G. Simpkins

The Boeing Company
Aero-Space Division
P. O. Box 3707
Seattle, Washington 98124
Attention: Ruth E. Peerenboom
Library Processes Supervisor

Celestial Research Corporation
1015 Fremont Avenue
South Pasadena, California 91030
Attention: Dr. Raymond L. Chuan

The Center for Research Libraries
5721 Cottage Grove Avenue
Chicago, Illinois 60637
Attention: Esther Smith
Acquisitions Librarian

Cornell Aeronautical Laboratory, Inc.
P. O Box 235
Buffalo, New York 14221
Attention: Mr. A. Hertzberg
Head, Aerodynamic Research
Attention: Library

General Dynamics/Fort Worth
P. O. Box 748
Fort Worth, Texas - 76101
Attention: Mr. R. C Frost
Aerospace Technology Section
Dept. 63-2
Mail Zone E-62
Attention: Mr. G. H Hull, P-54
Attention: Mr. A. P. Madsen
Chief, Aerospace Model Testing
Mail Zone P-54
Attention: Mr. Robert H. Widmer

General Dynamics/Astronautics
Space Sciences Laboratory
P. O. Box 1128
San Diego, California 92112
Attention: W. H. Gallagher
Mail Zone 596-30
Attention: Dr. Hideo Yoshihara
Mail Zone 583-00

General Dynamics/Daingerfield Division
Daingerfield, Texas 75638
Attention: Mr. J. E. McMichael
Chief, Jet Engine Department

General Electric Company (MSVD)
Space Technology Center
Space Sciences Laboratory
King of Prussia, Pennsylvania 19406
Attention: Dr. H. Lew

General Electric Company
Missile and Space Division
Valley Forge Space Technology Center
King of Prussia, Pennsylvania 19406
Attention: Library

General Electric Company
Research Laboratory
P. O. Box 1088
Schenectady, New York 12301
Attention: Dr. Henry T. Nagamatsu

Giannini Controls Corporation
1600 South Mountain Avenue
Duarte, California 91010
Attention: Library

Grumman Aircraft Engineering Corp.
Bethpage, Long Island, New
Attention: Mr. Charles Tilgner, Jr.
Director of Professional
Activities

Lockheed Georgia Company
Marietta, Georgia 30060
Attention: Dr. W. F. Jacobs
Aero-Space Technology
Department 72-08

Lockheed Missiles and Space Company
Research Laboratories
Technical Information Center
Department 50-14, Building 201
3251 Hanover Street
Palo Alto, California 94304
Attention: Dr. W. A. Kozumplik

Lockheed Missiles and Space Company
Engineering - Research and Development
P. O. Box 504
Sunnyvale, California 94088
Attention: Mr. Maurice Tucker

Marquhardt Aircraft Company
16555 Saticoy Street
Van Nuys, California 91406
Attention: Library

The Martin Company
Baltimore, Maryland 21233
Attention: Mr. K. Jarmolow
Mail No. J-3033

McDonnell Aircraft Corporation
P. O. Box 516
St. Louis, Missouri 63166
Attention: Engineering Library
Department 218

McDonnell-Douglas Corporation
3000 Ocean Park Blvd.
Santa Monica, California 90405
Attention: Dr. R. J. Hakkinen
Chief Scientist
Physical Sciences Dept.
Attention: Chief, Astrodynamics Branch,
AST (A-260)

McDonnell-Douglas Corporation
Douglas Aircraft Division
3855 Lakewood Blvd.
Long Beach, California 90808
Attention: Dr. A. M. O. Smith

North American Aviation, Inc.
Space and Information Systems Division
Apollo Management
12214 Lakewood Blvd.
Downey, California 90241
Attention: Dr. John F. McCarthy, Jr.

The RAND CORPORATION
1700 Main Street
Santa Monica, California 90401
Attention: Dr. Carl Gazley, Jr.

Republic Aviation Corporation
Farmingdale, Long Island, New York 11735
Attention: Engineering Library

Space Sciences, Inc.
301 Bear Hill Rd.
Waltham, Massachusetts 02154
Attention: Pung Nien Hu
Principal Scientist

TRW Systems
One Space Park
Redondo Beach, California 90278
Attention: Library
Attention: Dr. R. G. Batt
Bldg. R-4, Room 2036
Attention: Dr. James E. Broadwell
Aerosciences Laboratory
Research Staff
Attention: Dr. C. B. Cohen
Attention: Dr. A. G. Hammitt, Manager
Aerosciences Laboratory
Research Staff
Attention: Dr. John E. Lewis
Bldg. R-4, Room 2050
Attention: Dr. Arvel B. Witte
Bldg. R-4, Room 2050